Antikinetoplastid SAR study in 3-nitroimidazopyridine series: identification of a novel non-genotoxic and potent anti-*T. b. brucei* hit-compound with improved pharmacokinetic properties.

Cyril Fersing[1#], Clotilde Boudot[2#], Romain Paoli-Lombardo[1], Nicolas Primas[1], Emilie Pinault[3], Sébastien Hutter[4], Caroline Castera-Ducros[1], Youssef Kabri[1], Julien Pedron[5], Sandra Bourgeade-Delmas[6], Alix Sournia-Saquet[5], Jean-Luc Stigliani[5], Alexis Valentin[6], Amaya Azqueta[7], Damián Muruzabal[7], Alexandre Destere[8], Susan Wyllie[9], Alan H. Fairlamb[9], Sophie Corvaisier[10], Marc Since[10], Aurélie Malzert-Fréon[10], Carole Di Giorgio[11], Pascal Rathelot[1], Nadine Azas[4], Bertrand Courtioux[2], Patrice Vanelle[1] and Pierre Verhaeghe[5*].

[1] Aix Marseille Univ, CNRS, ICR UMR 7273, Equipe Pharmaco-Chimie Radicalaire, Faculté de Pharmacie, 27 Boulevard Jean Moulin, CS30064, 13385, Marseille Cedex 05, France.

[2] Université de Limoges, UMR Inserm 1094, Neuroépidémiologie Tropicale, Faculté de Pharmacie, 2 rue du Dr Marcland, 87025 Limoges, France.

[3] Université de Limoges, BISCEm, US 042 INSERM – UMS 2015 CNRS, Mass Spectrometry Platform, CBRS, 2 rue du Pr. Descottes, F-87025 Limoges, France.

[4] Aix Marseille Univ, IHU Méditerranée Infection, UMR VITROME - Tropical Eukaryotic Pathogens, 19-21 Boulevard Jean Moulin, 13005 Marseille, France.

[5] LCC-CNRS Université de Toulouse, CNRS, UPS, Toulouse, France.

[6] UMR 152 PHARMA-DEV, Université de Toulouse, IRD, UPS, Toulouse, France.

[7] Department of Pharmacology and Toxicology, Faculty of Pharmacy and Nutrition, University of Navarra, C/ Irunlarrea 1, CP 31008, Pamplona, Navarra, Spain.

[8] Department of Pharmacology, Toxicology and Pharmacovigilance, CHU Limoges, Limoges, France, INSERM, UMR 1248, University of Limoges, France.

[9] University of Dundee, School of Life Sciences, Division of Biological Chemistry and Drug Discovery, Dow Street, Dundee DD1 5EH, Scotland, United Kingdom.

[10] Normandie Univ, UNICAEN, CERMN, 14000 Caen, France.

[11] Institut Méditerranéen de Biodiversité et d'Ecologie marine et continentale (IMBE), Aix-Marseille Université, UMR CNRS IRD Avignon Université, Campus Timone – Faculté de Pharmacie, 27 boulevard Jean-Moulin, F13385 Marseille cedex 05.

Supplementary material

Table of content

1. Experimental spectra

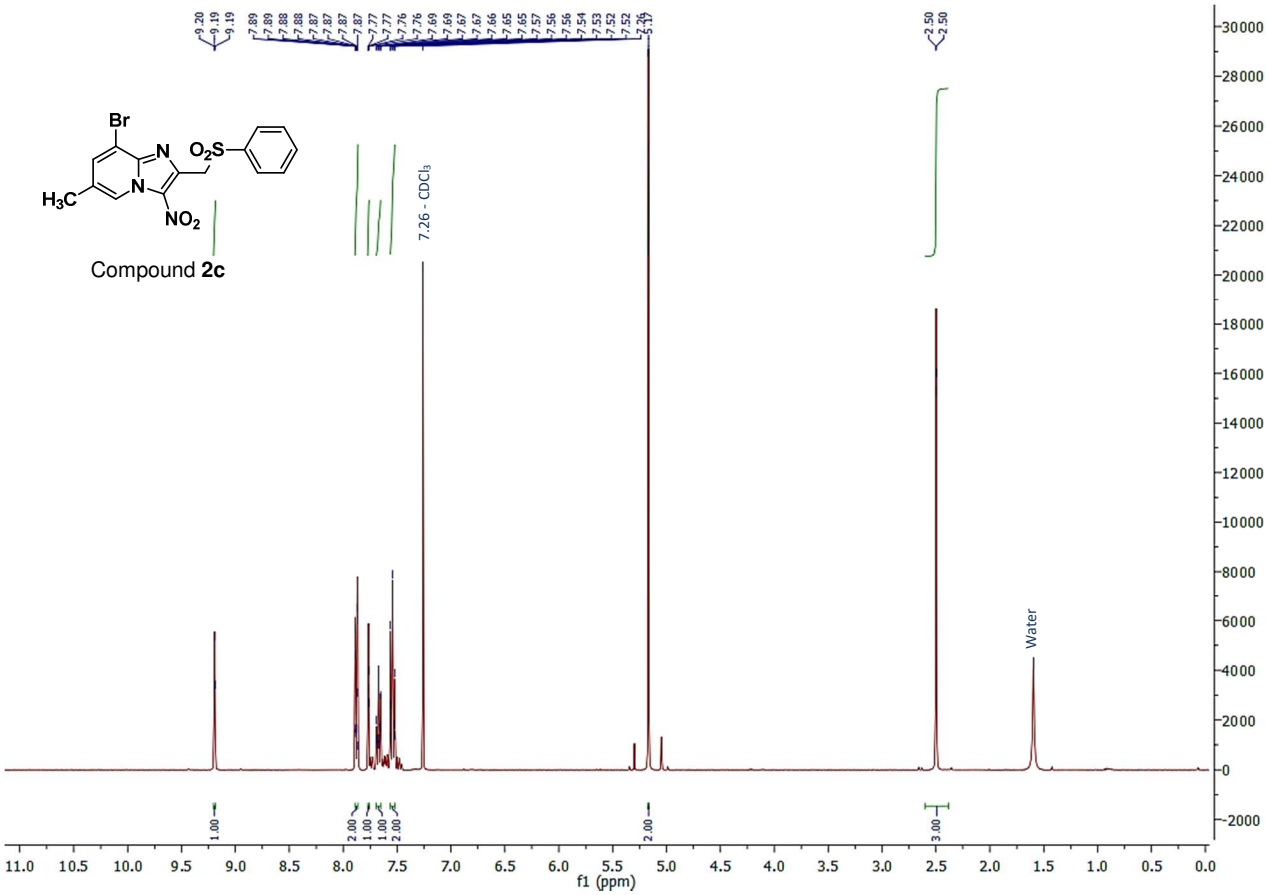

Figure S1 – ^{1}H NMR spectrum of **2c** in $CDCl_3$, on a Bruker ARX 200 spectrometer.

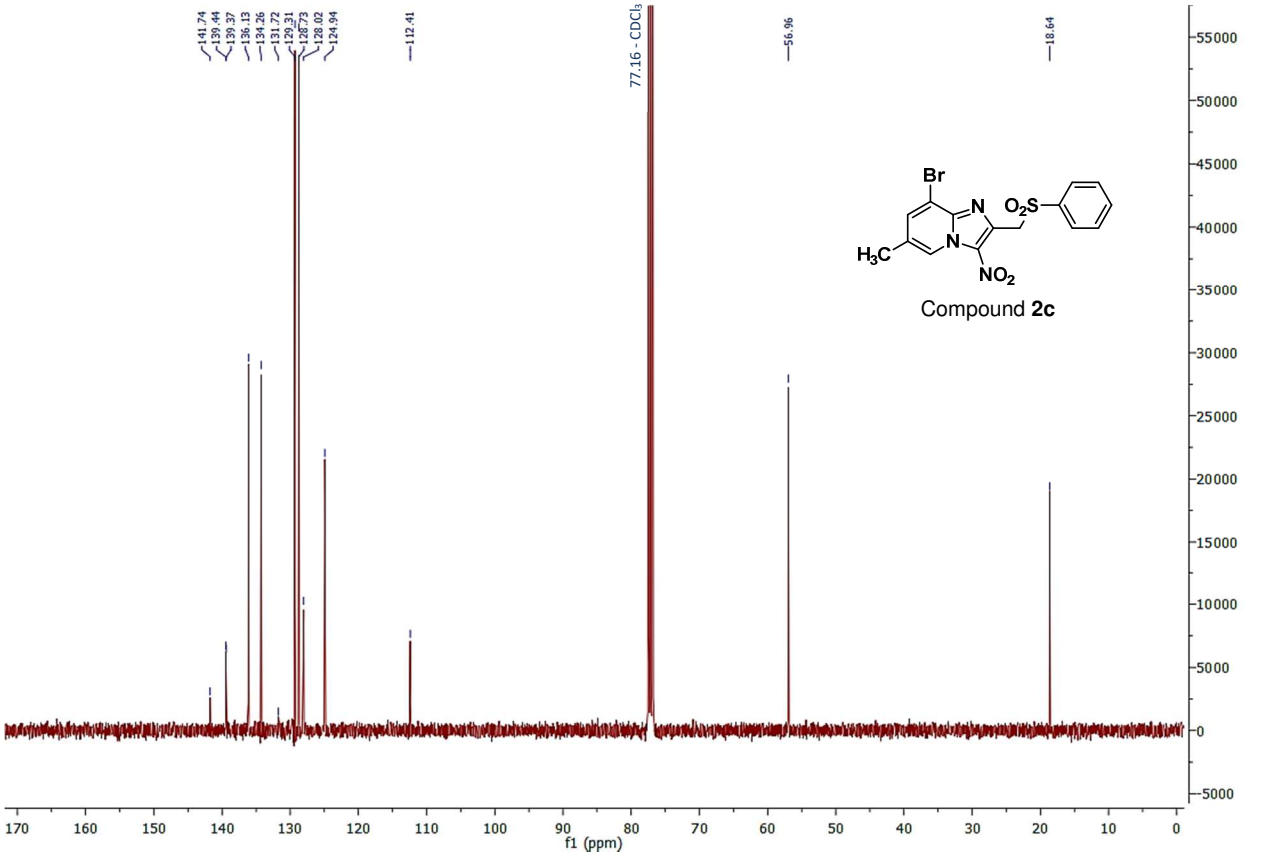

Figure S2 – ^{13}C NMR spectrum of **2c** in $CDCl_3$, on a Bruker ARX 200 spectrometer.

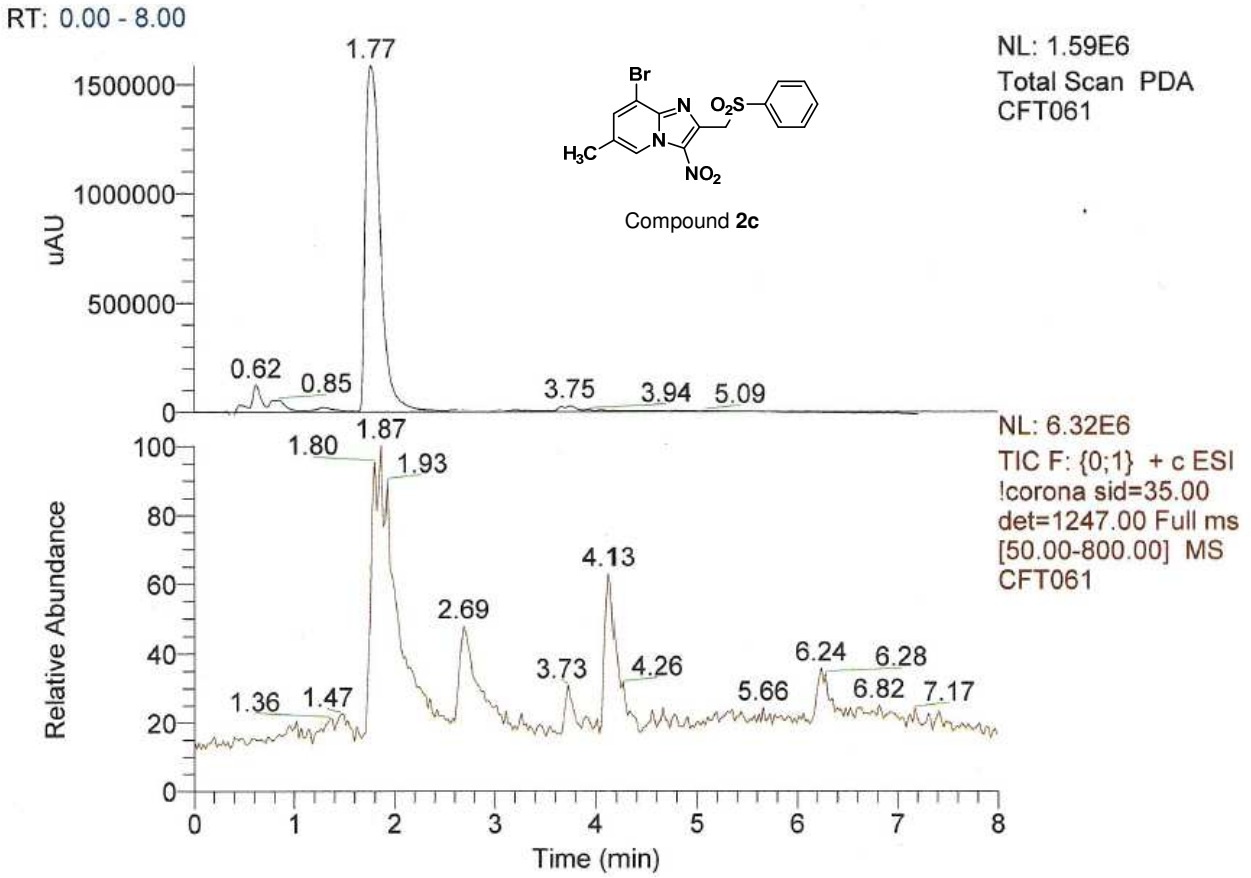

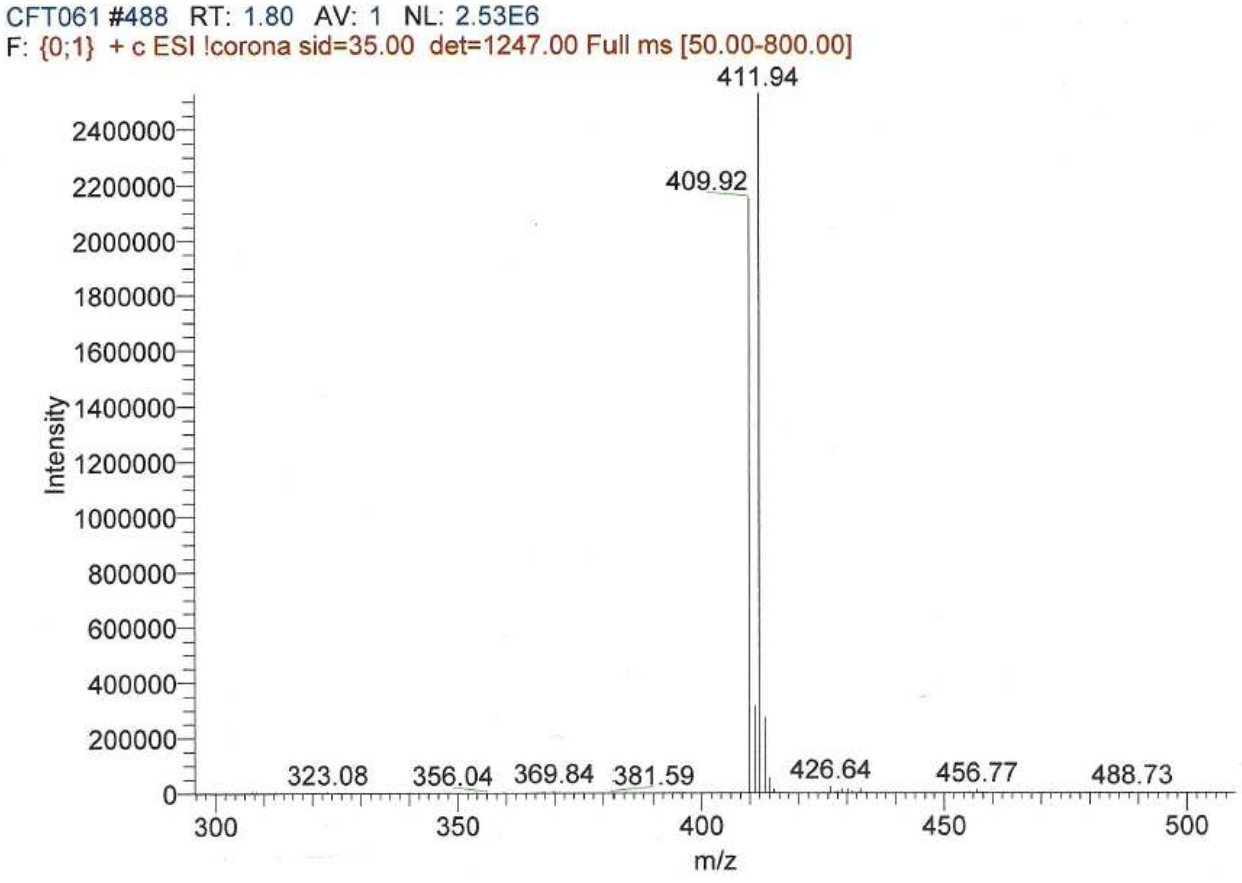

Figure S3 – LC/MS spectrum of compound **2c**.

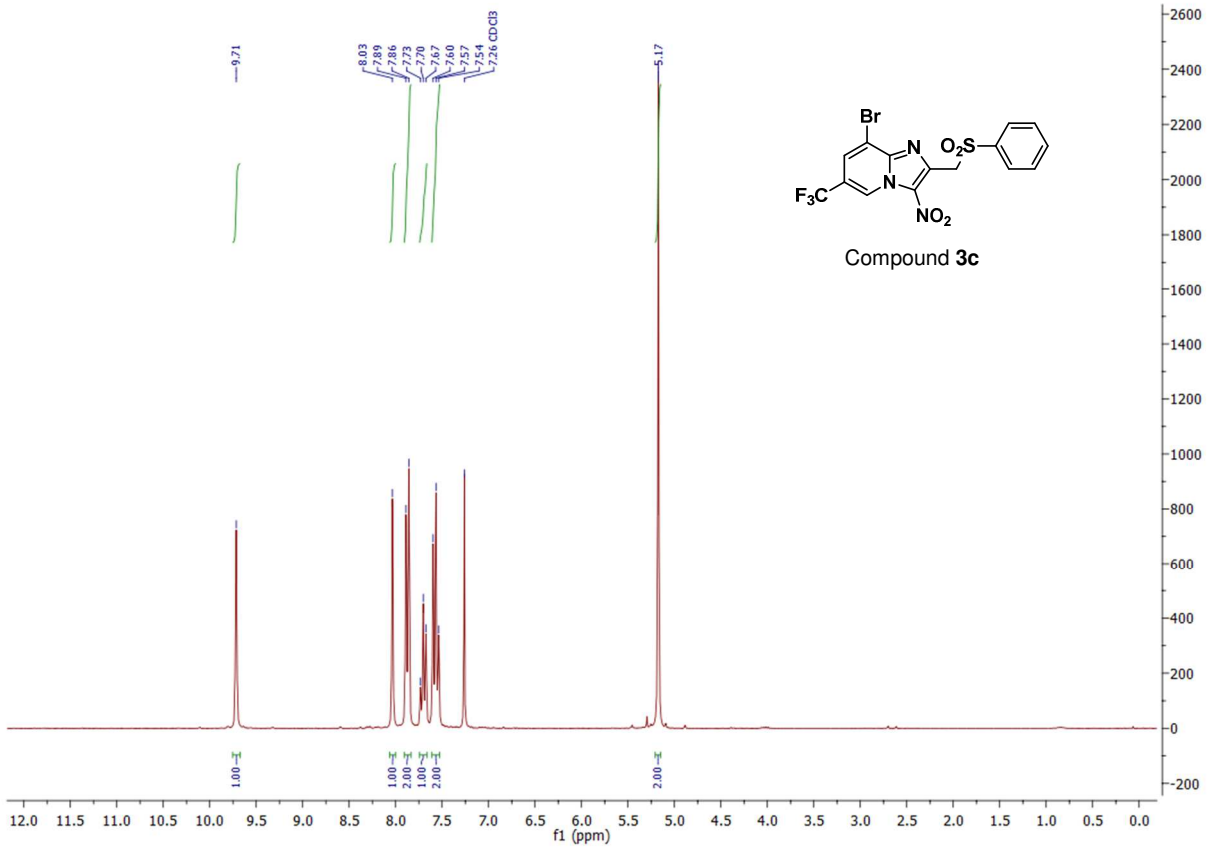

Figure S4 – ^{1}H NMR spectrum of **3c** in $CDCl_3$, on a Bruker ARX 200 spectrometer.

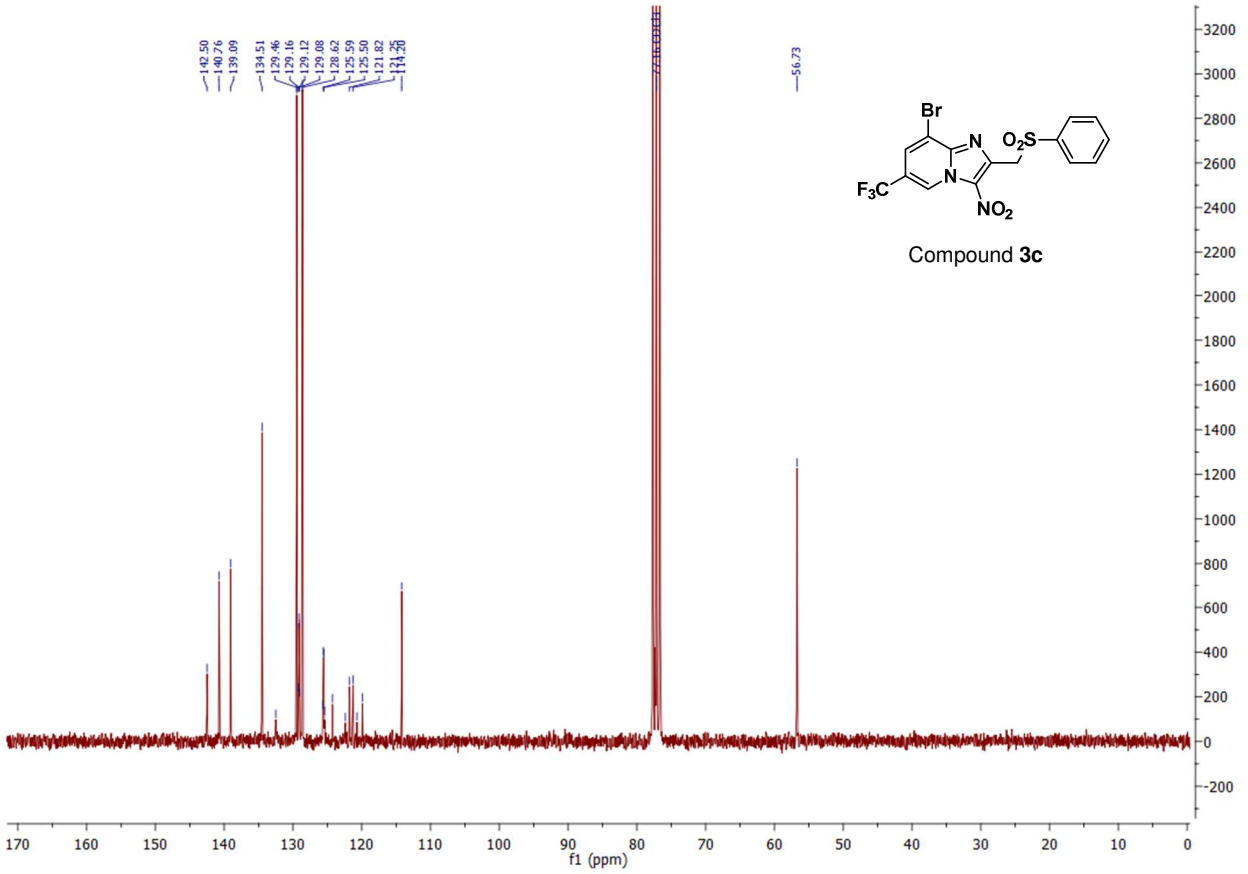

Figure S5 – ^{13}C NMR spectrum of **3c** in $CDCl_3$, on a Bruker ARX 200 spectrometer.

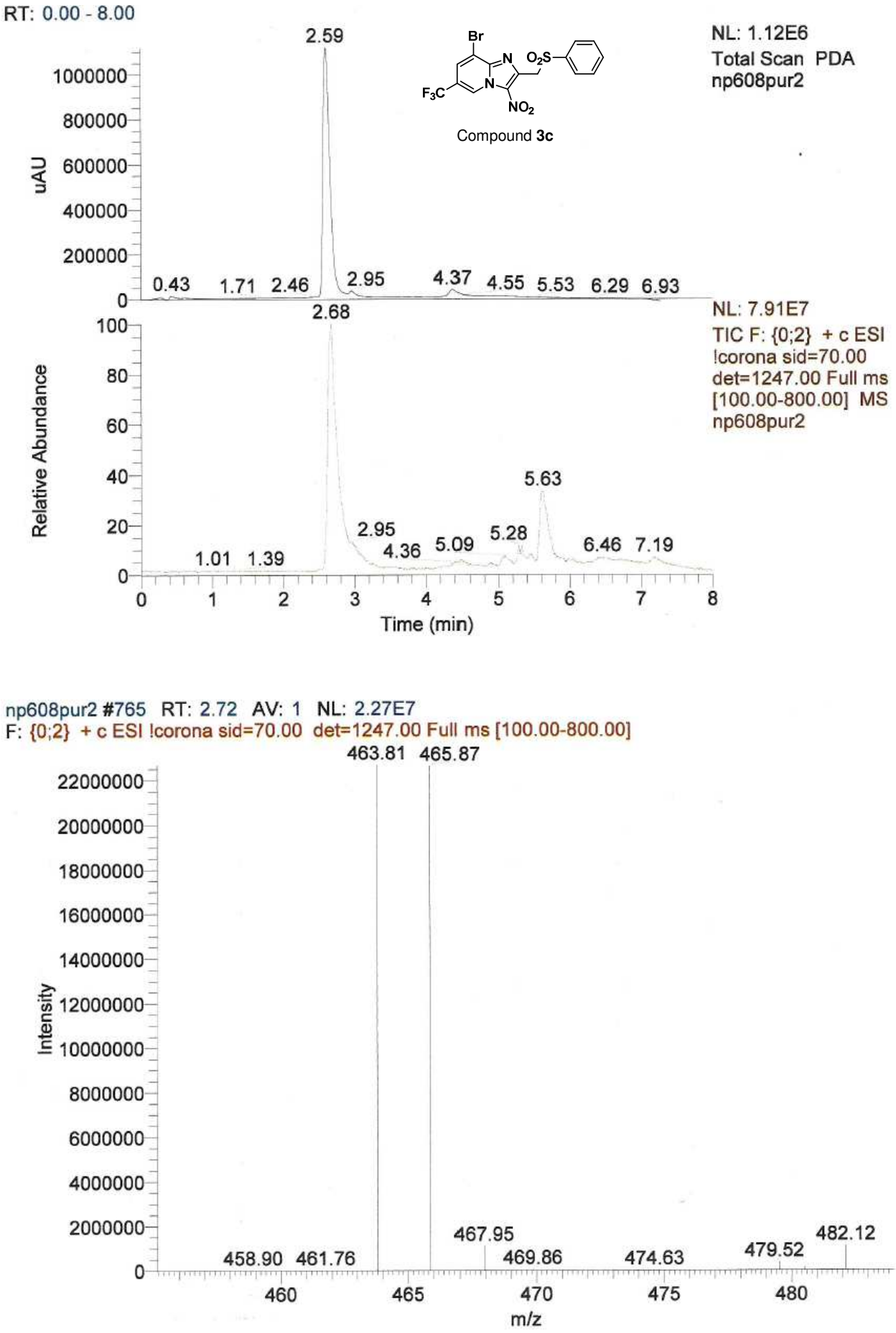

Figure S6 – LC/MS spectrum of compound **3c**.

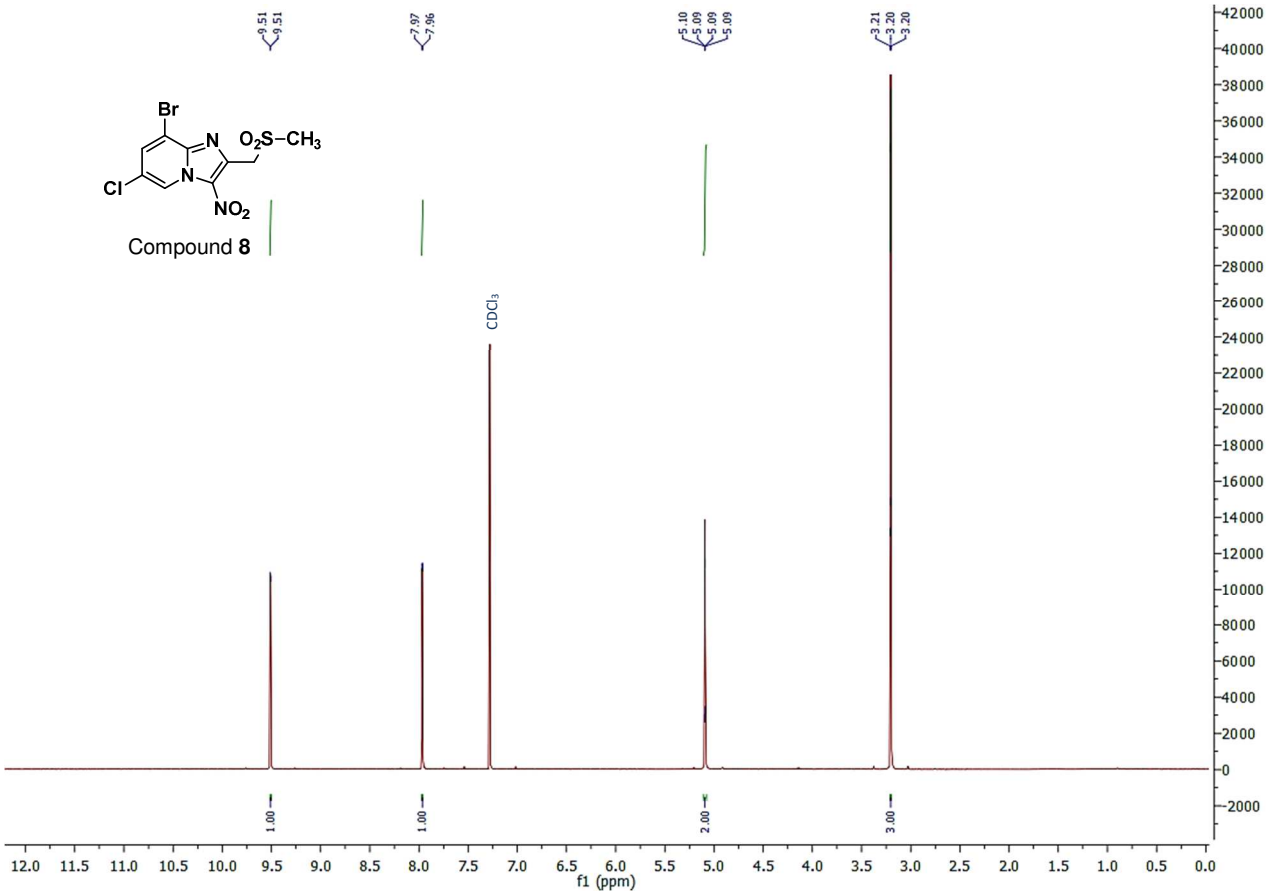

Figure S7 – ^{1}H NMR spectrum of **8** in $CDCl_3$, on a Bruker Avance III nanobay 400 spectrometer.

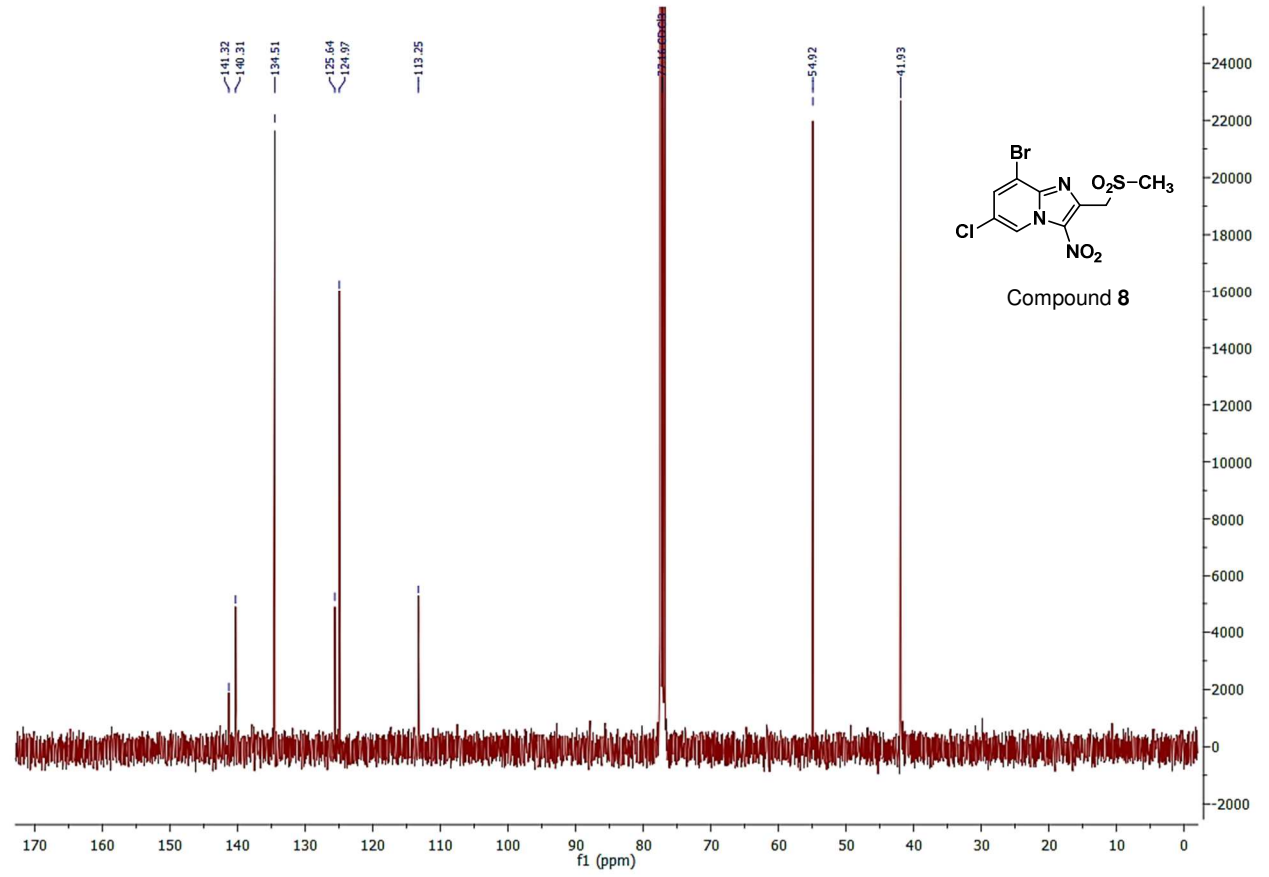

Figure S8 – ^{13}C NMR spectrum of **8** in $CDCl_3$, on a Bruker Avance III nanobay 400 spectrometer.

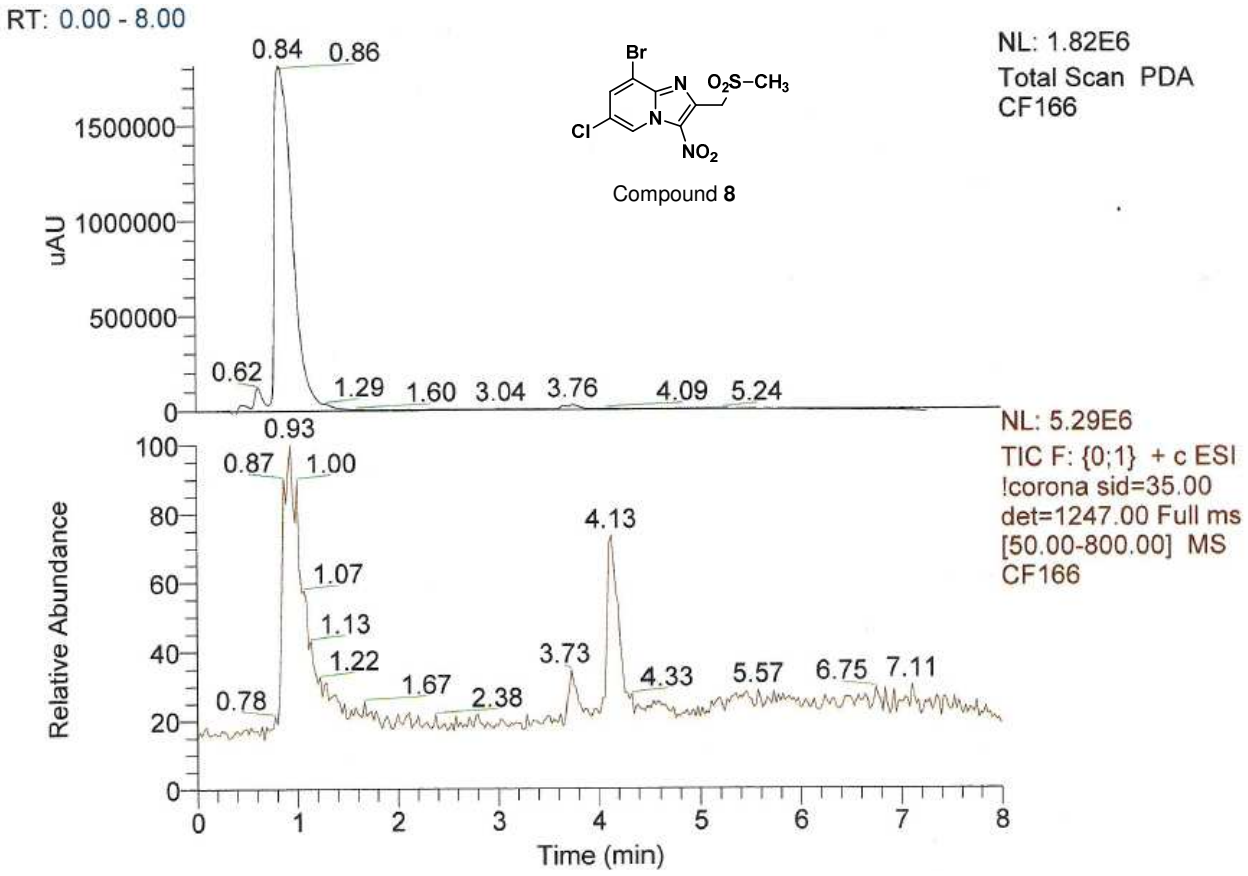

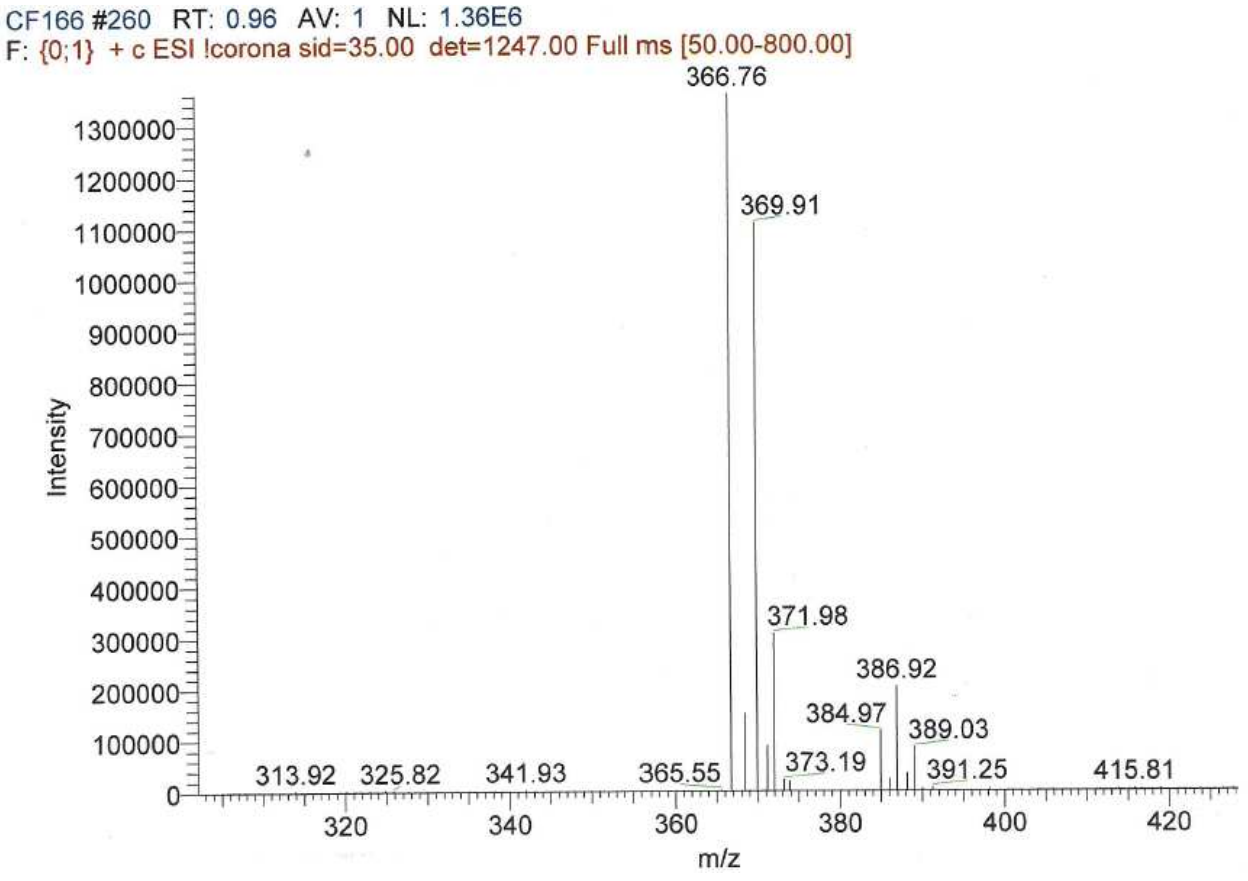

Figure S9 – LC/MS spectrum of compound **8**.

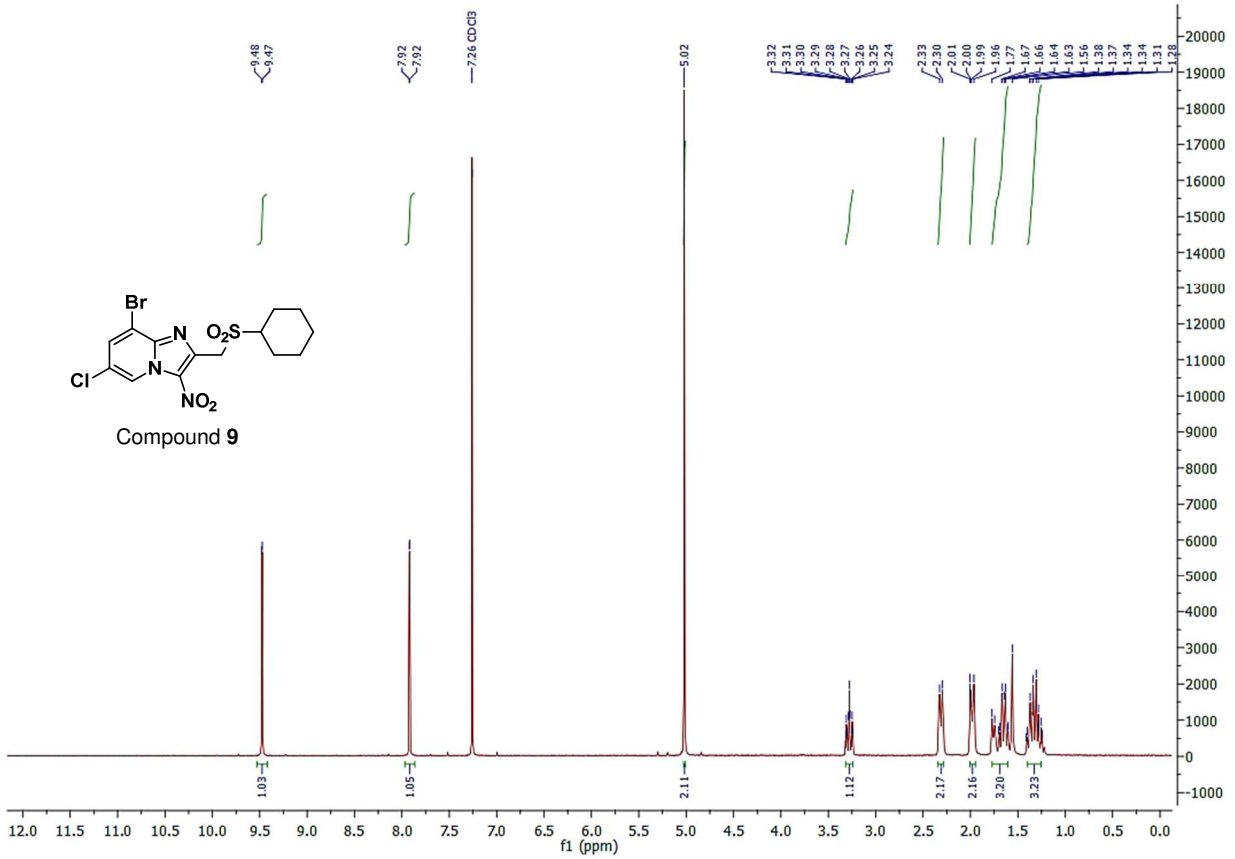

Figure S10 – ^{1}H NMR spectrum of **9** in $CDCl_3$, on a Bruker Avance III nanobay 400 spectrometer.

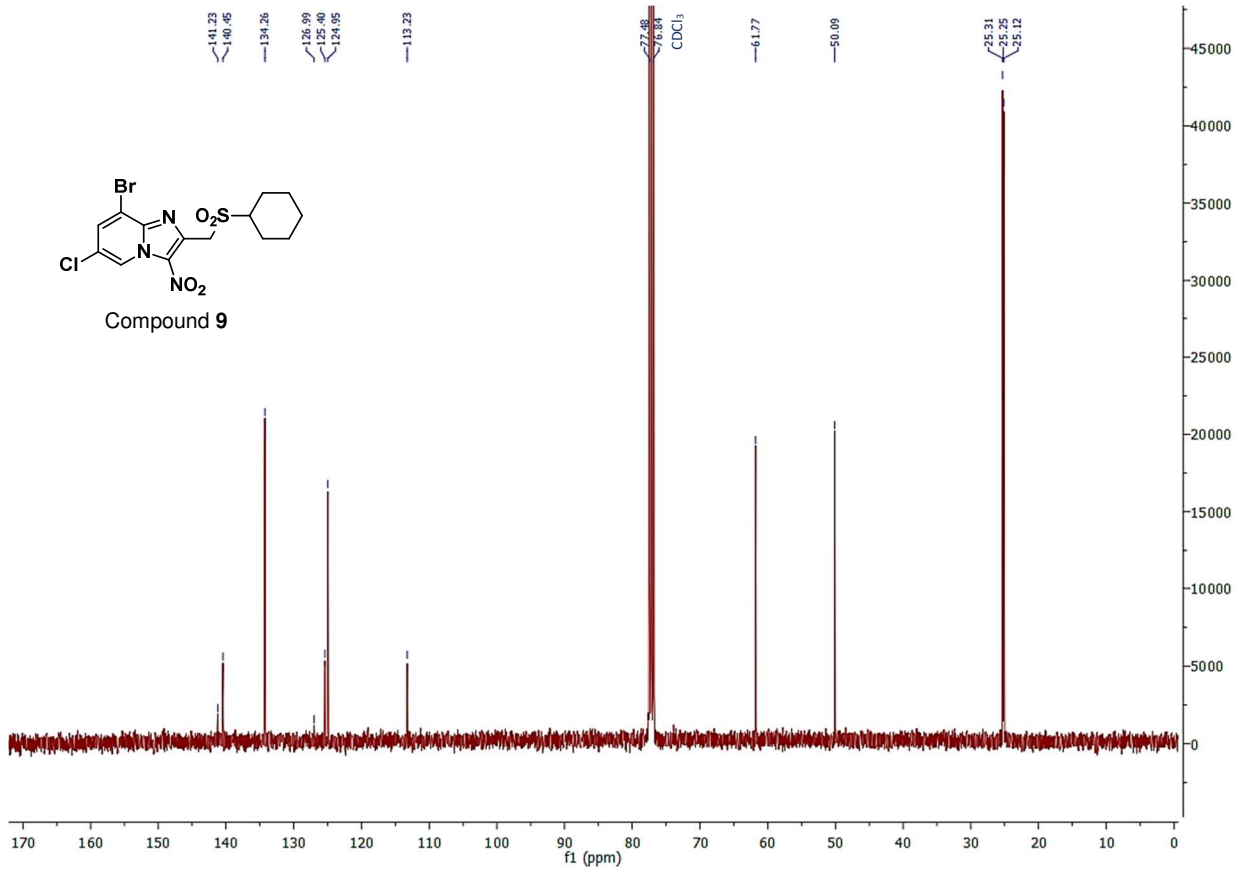

Figure S11 – ^{13}C NMR spectrum of **9** in $CDCl_3$, on a Bruker Avance III nanobay 400 spectrometer.

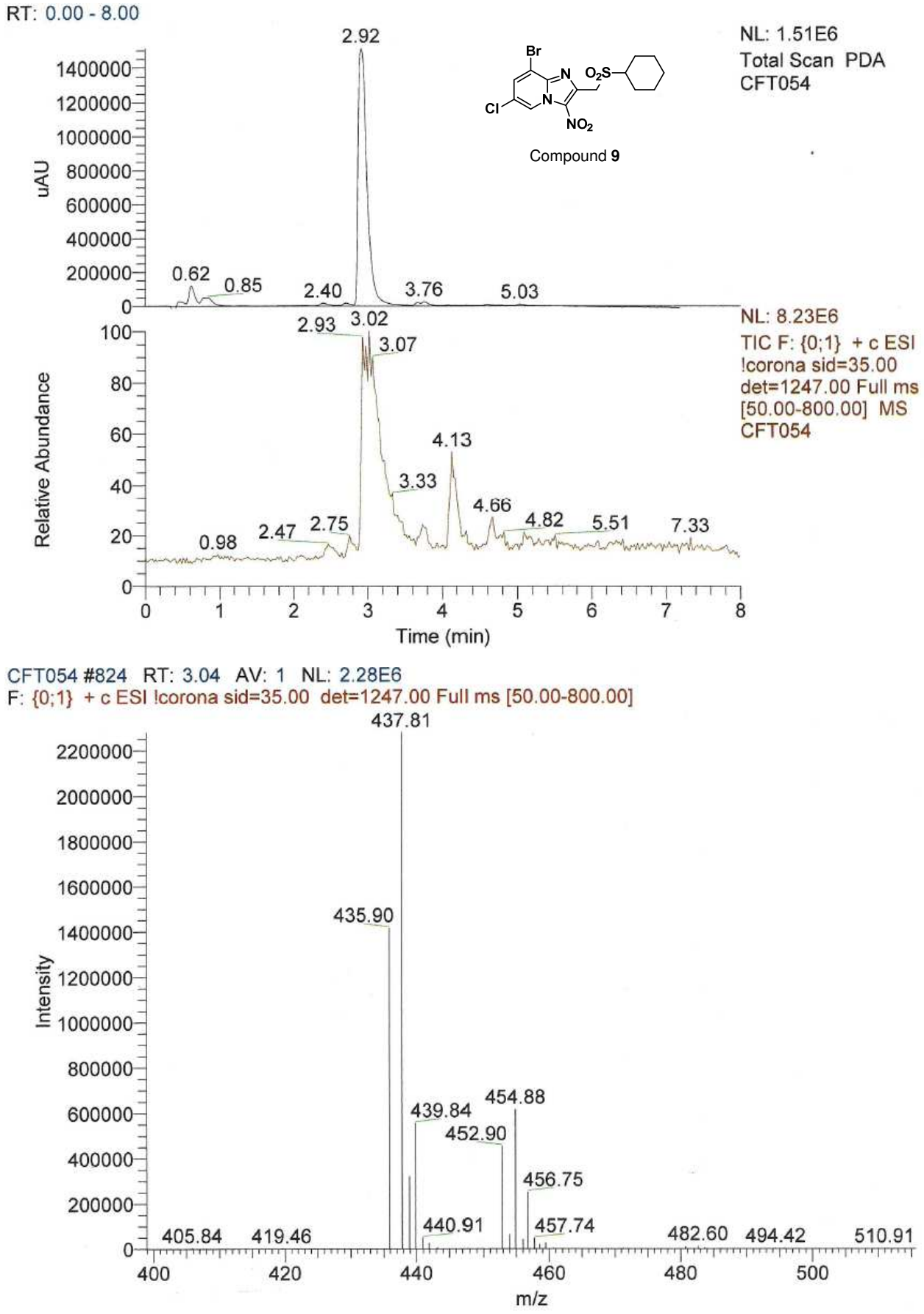

Figure S12 – LC/MS spectrum of compound **9**.

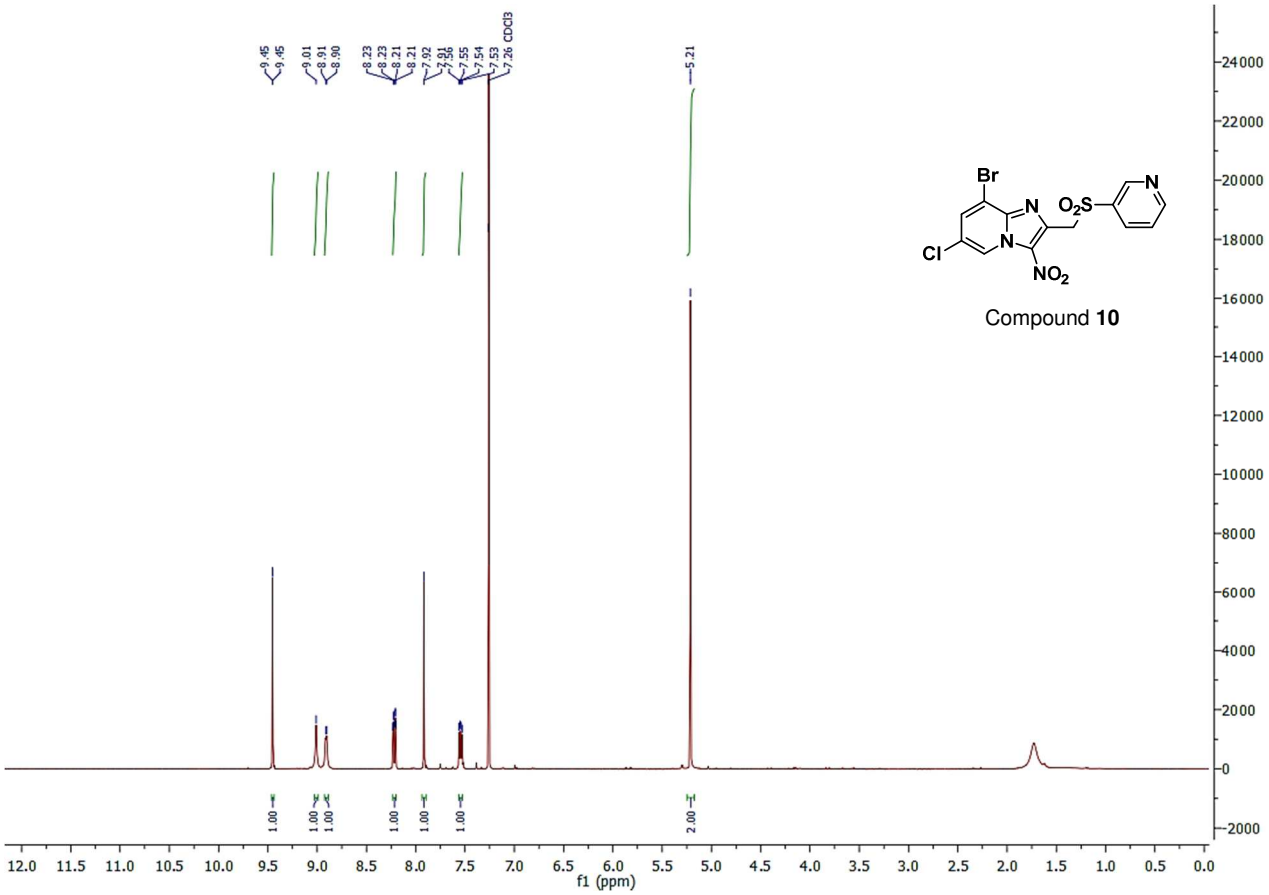

Figure S13 – ^{1}H NMR spectrum of **10** in $CDCl_3$, on a Bruker Avance III nanobay 400 spectrometer.

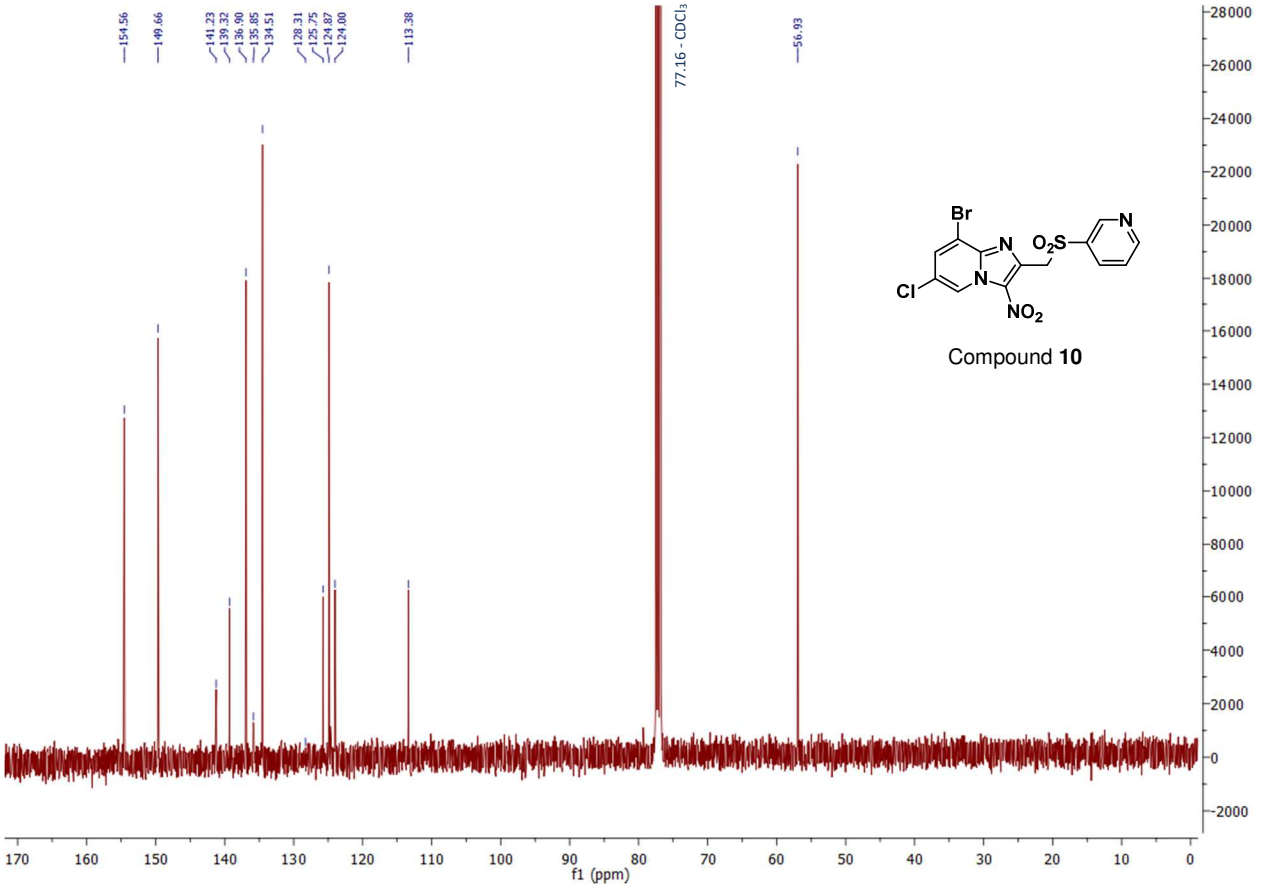

Figure S14 – ^{13}C NMR spectrum of **10** in $CDCl_3$, on a BRUKER Avance III nanobay 400 spectrometer.

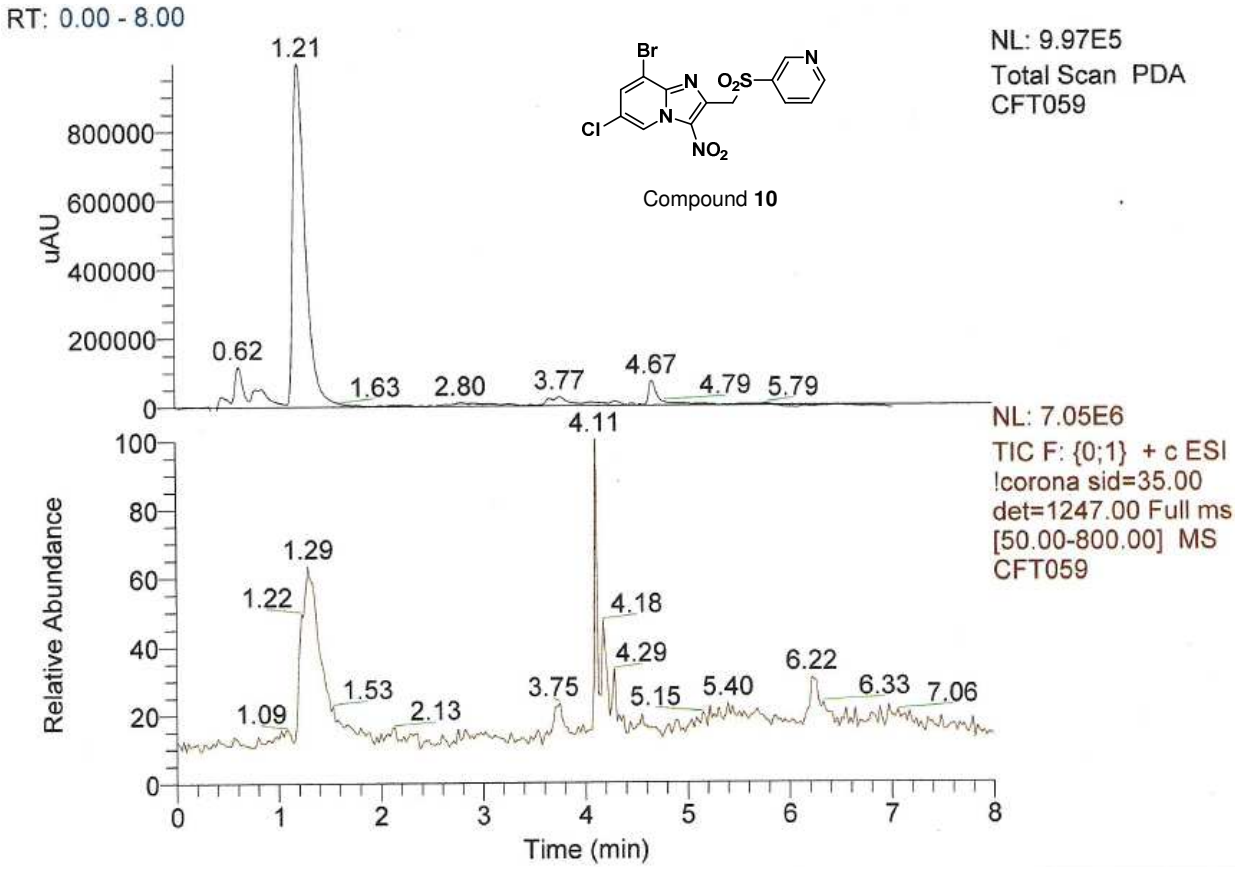

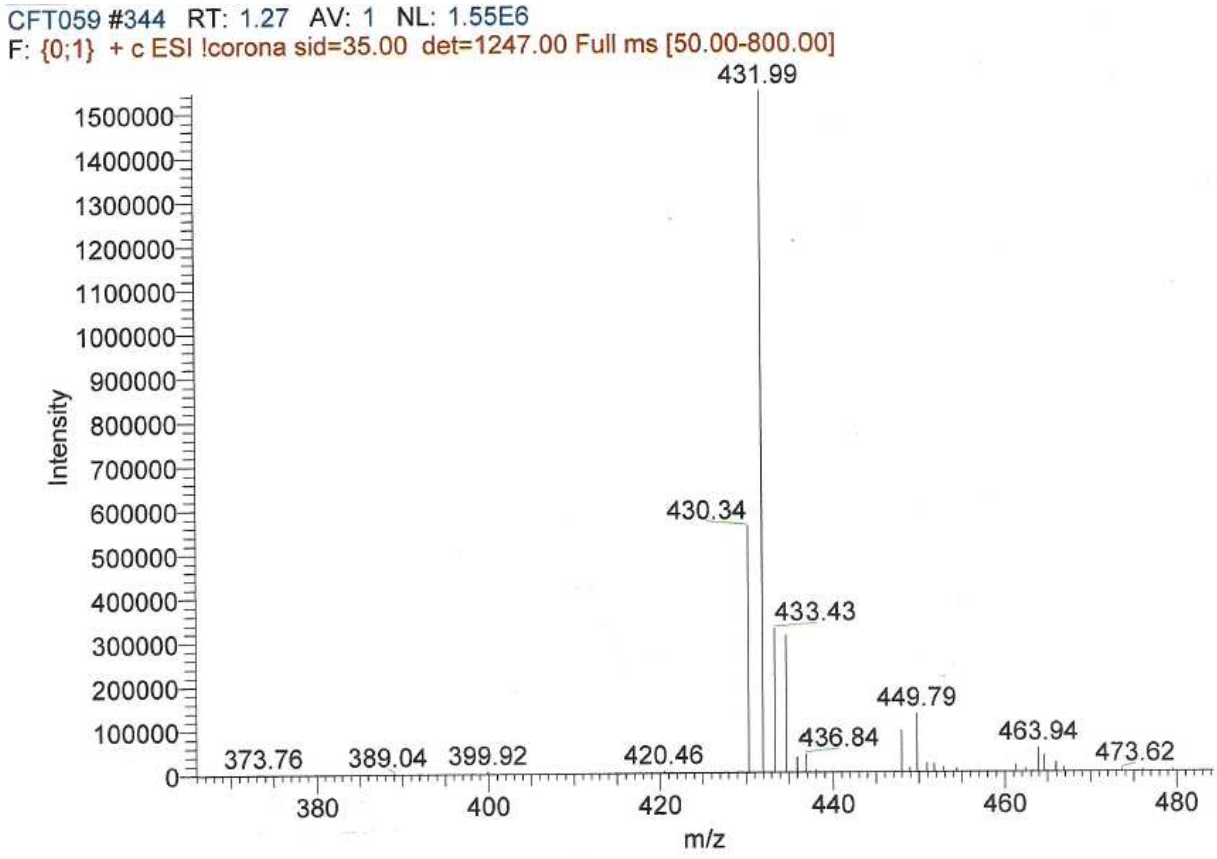

Figure S15 – LC/MS spectrum of compound **10**.

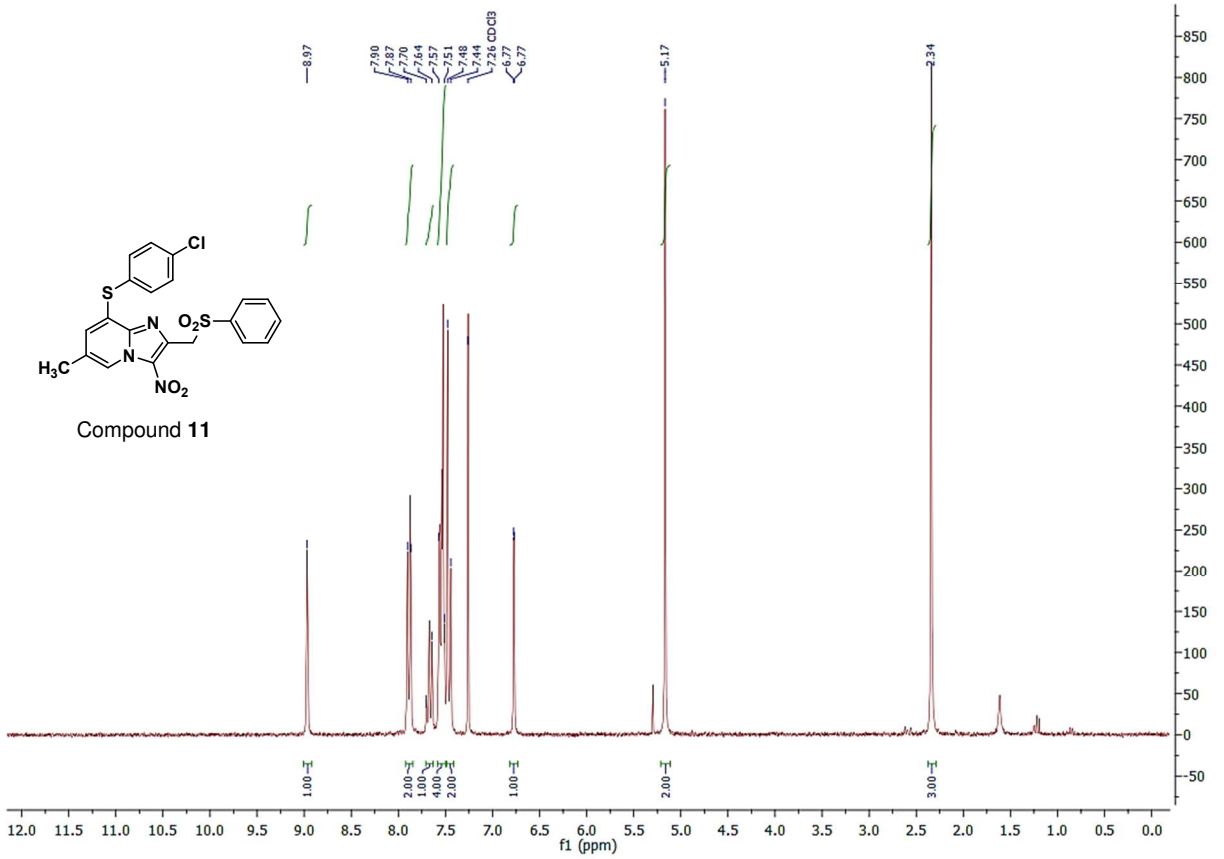

Figure S16 – ^{1}H NMR spectrum of **11** in $CDCl_3$, on a Bruker ARX 200 spectrometer.

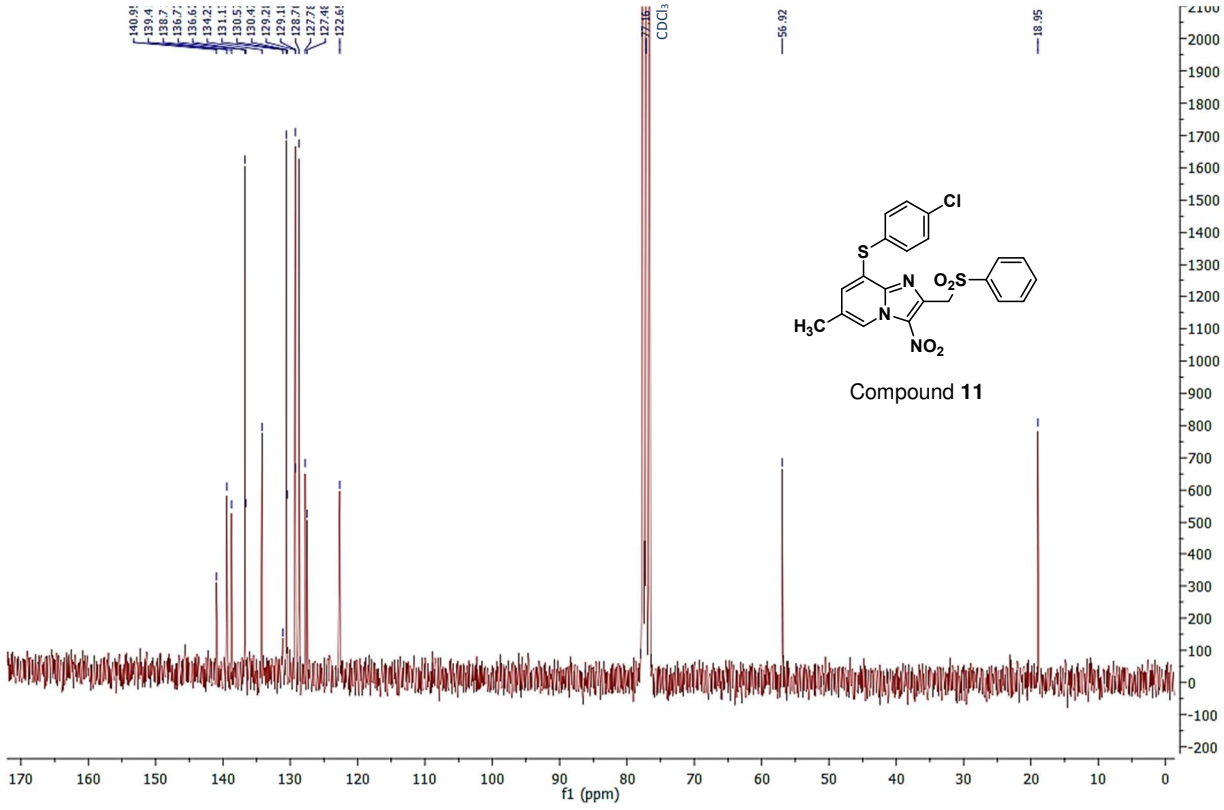

Figure S17 – ^{13}C NMR spectrum of **11** in $CDCl_3$, on a Bruker ARX 200 spectrometer.

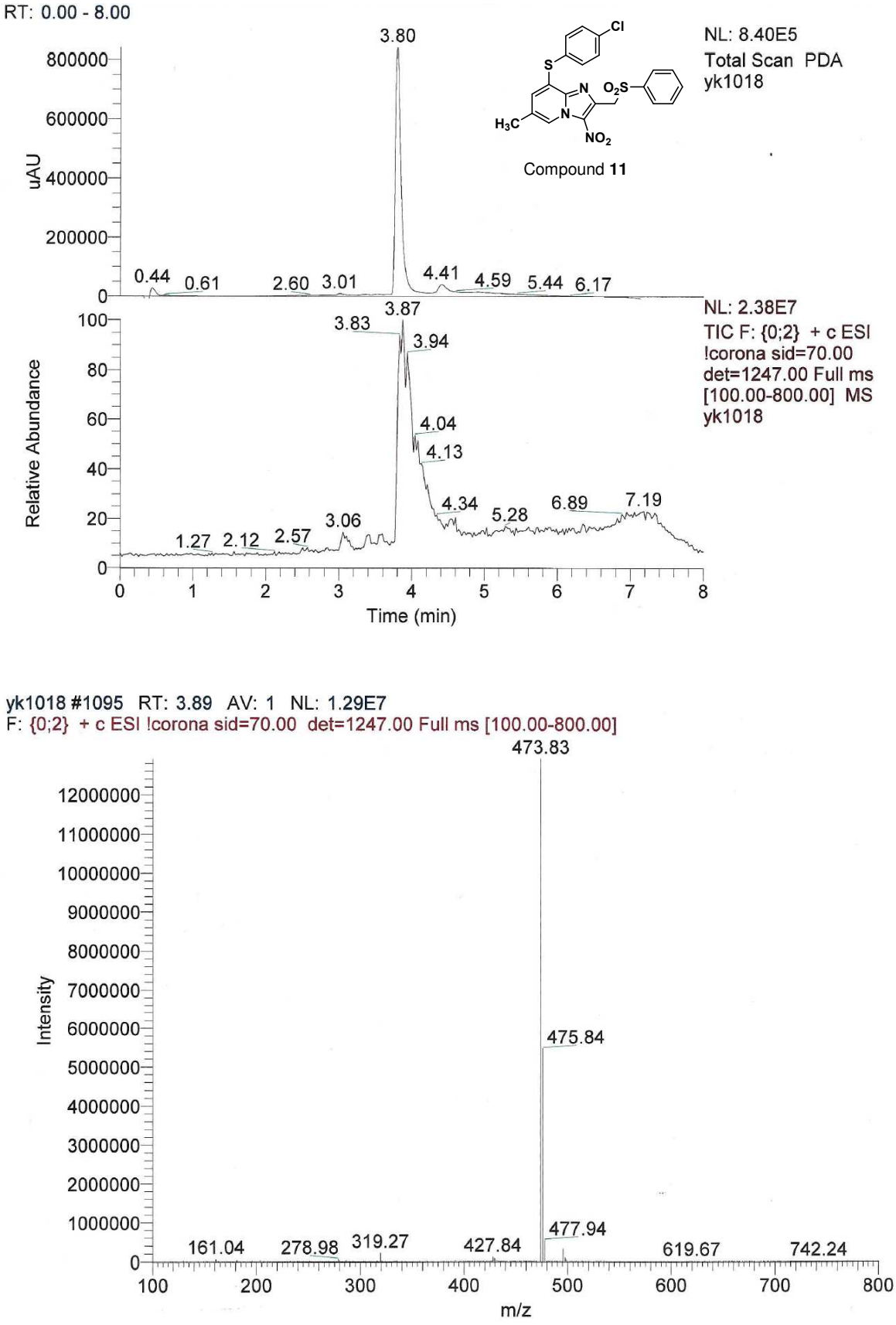

Figure S18 – LC/MS spectrum of compound **11**.

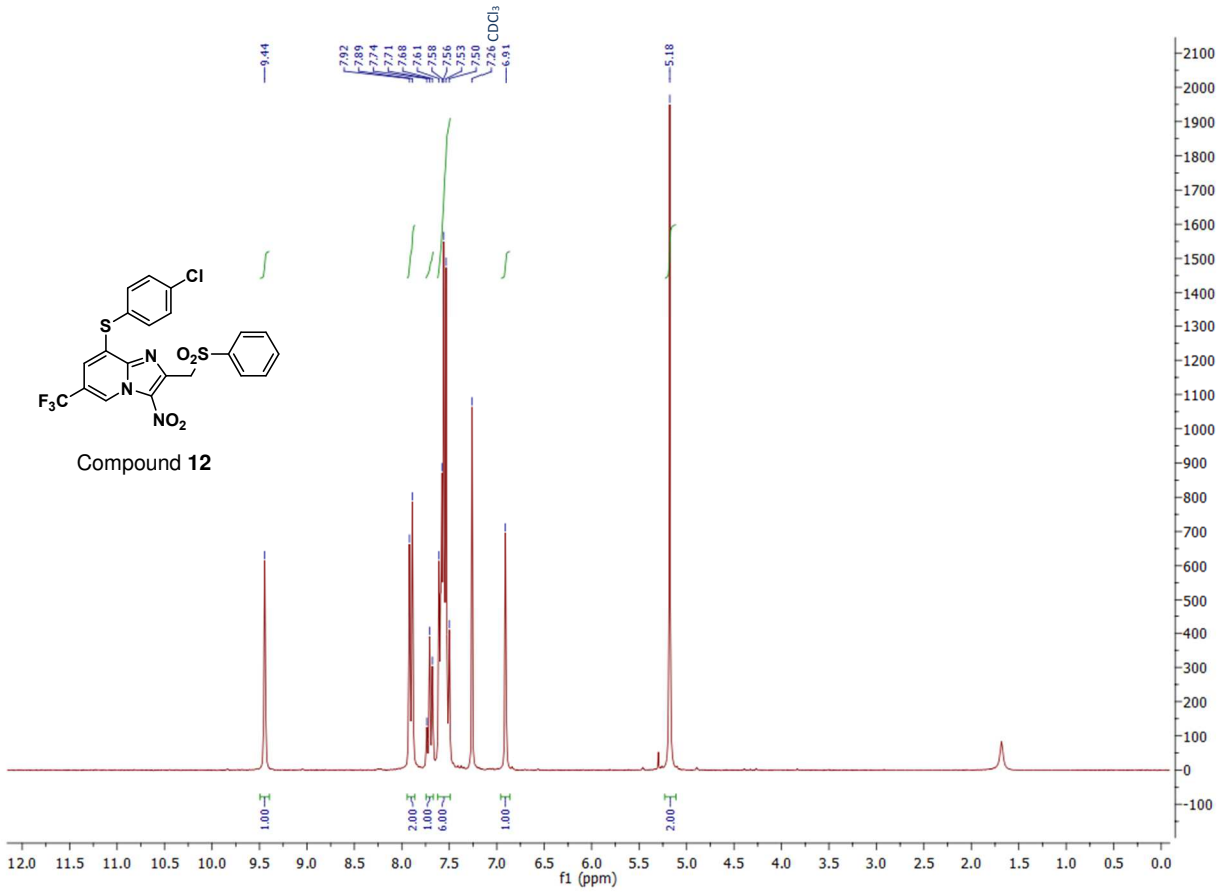

Figure S19 – ^{1}H NMR spectrum of **12** in $CDCl_3$, on a Bruker AV 250 spectrometer.

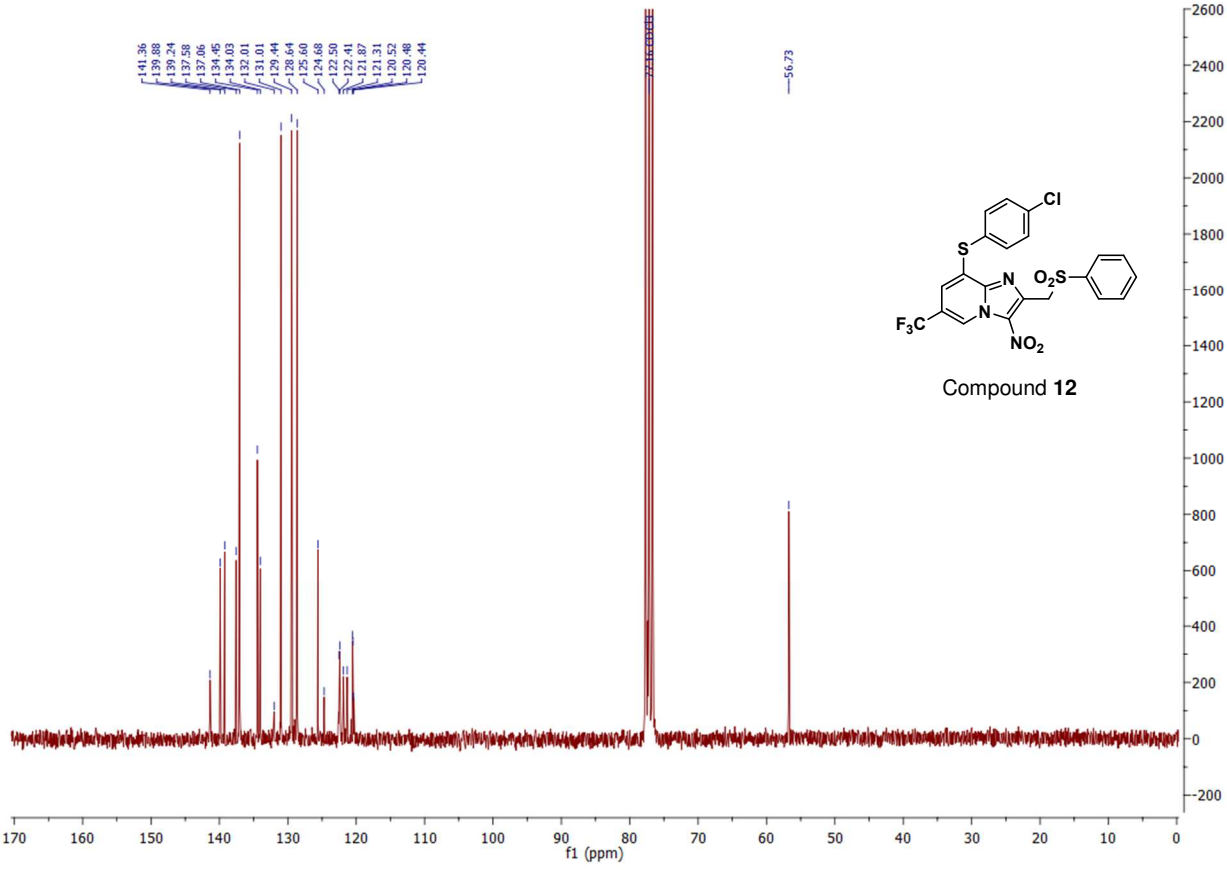

Figure S20 – ^{13}C NMR spectrum of **12** in $CDCl_3$, on a Bruker AV 250 spectrometer.

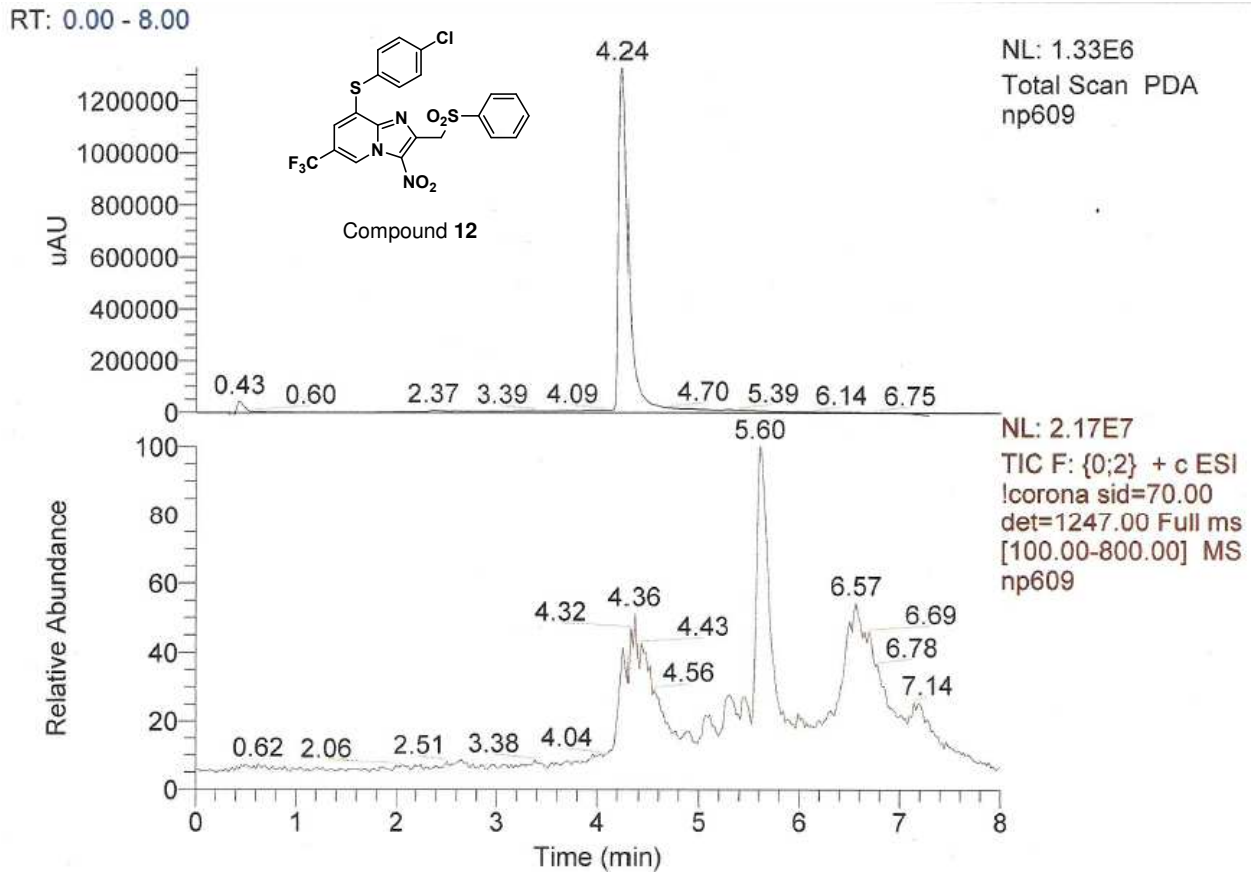

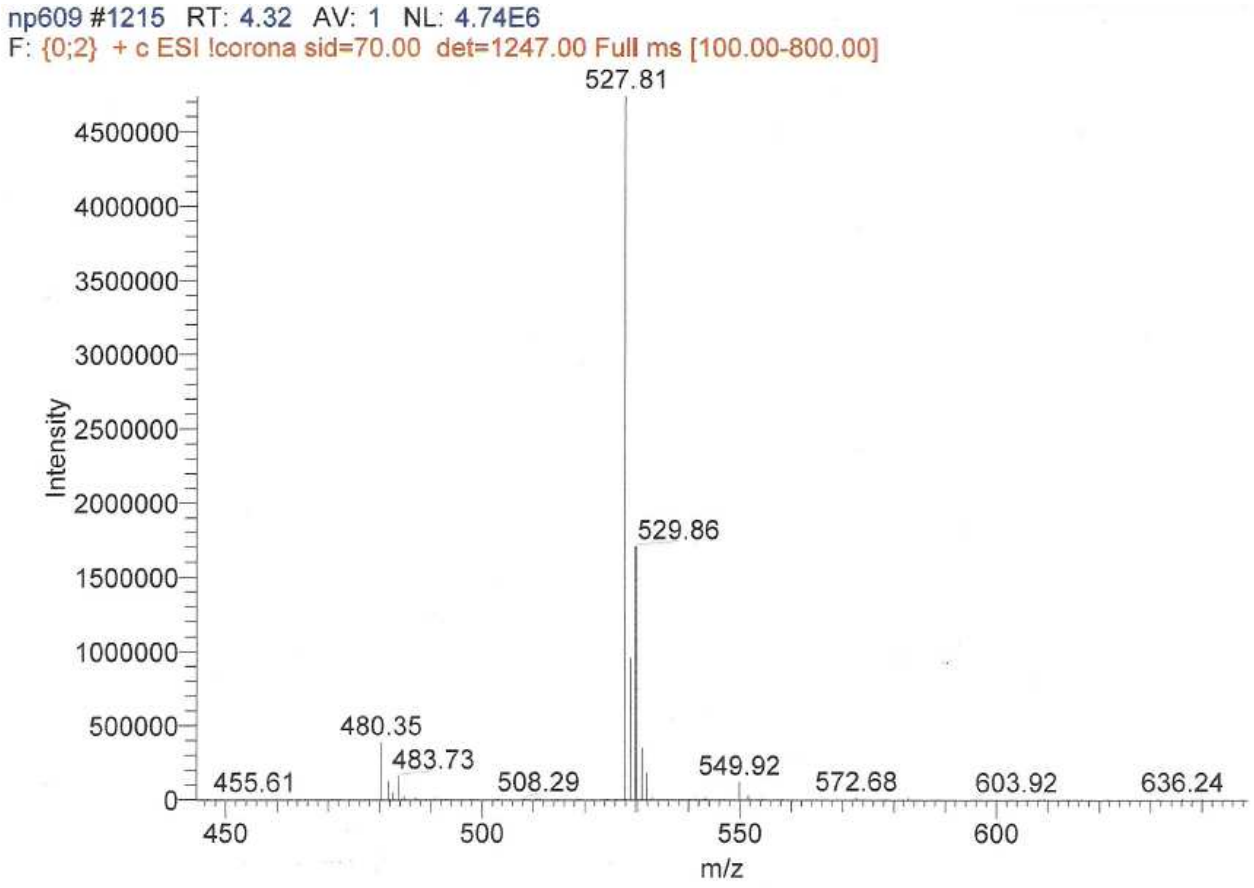

Figure S21 – LC/MS spectrum of compound **12**.

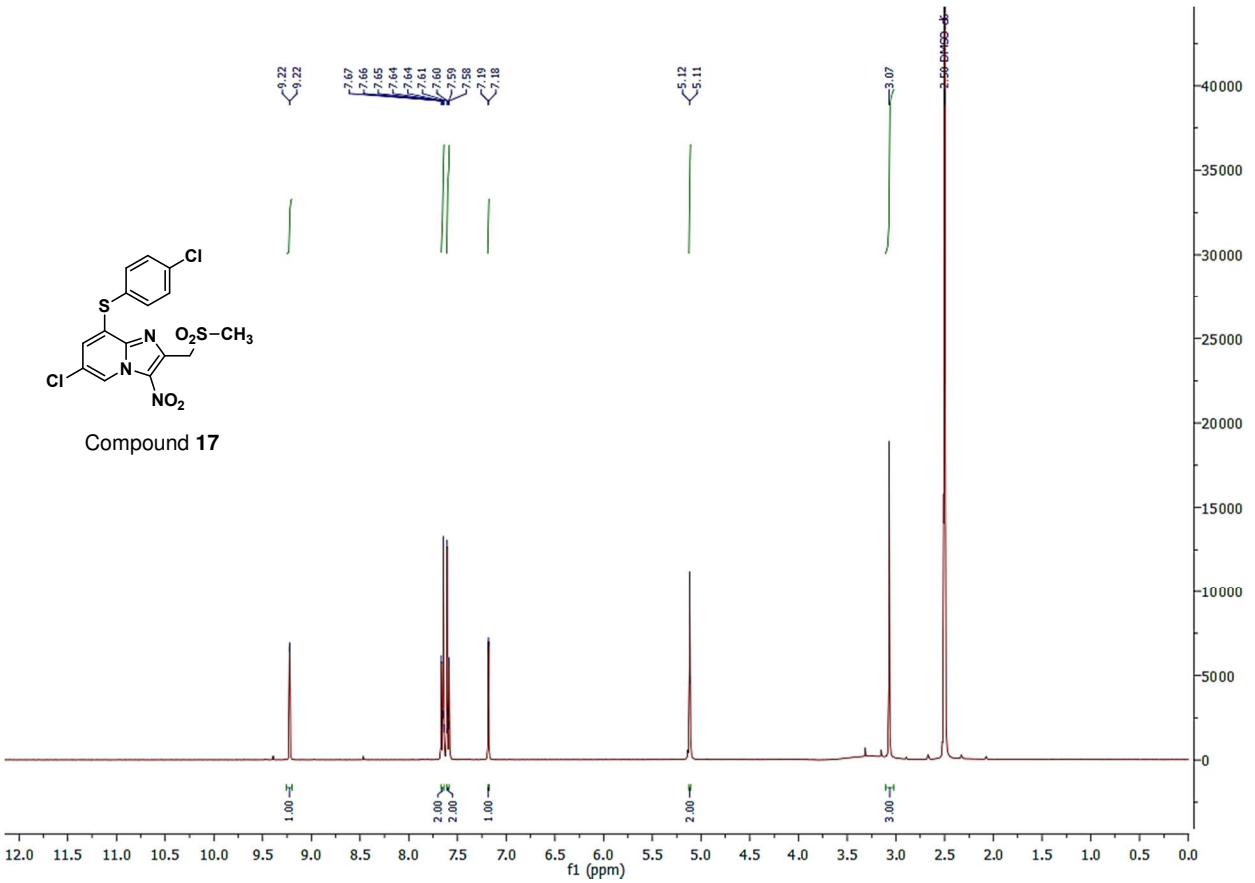

Figure S22 – ^{1}H NMR spectrum of **17** in DMSO-d_6, on a Bruker Avance III nanobay 400.

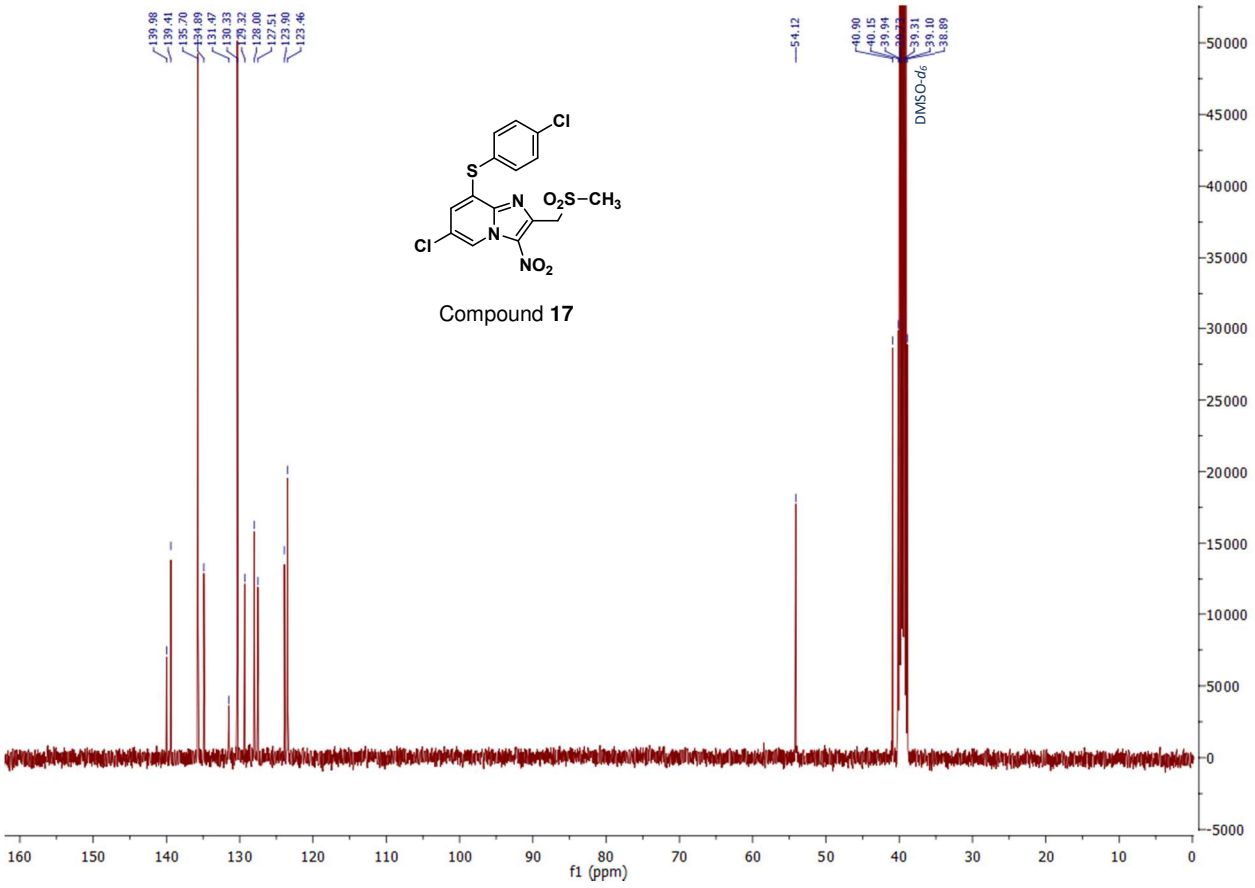

Figure S23 – ^{13}C NMR spectrum of **17** in DMSO-d_6, on a Bruker Avance III nanobay 400 spectrometer.

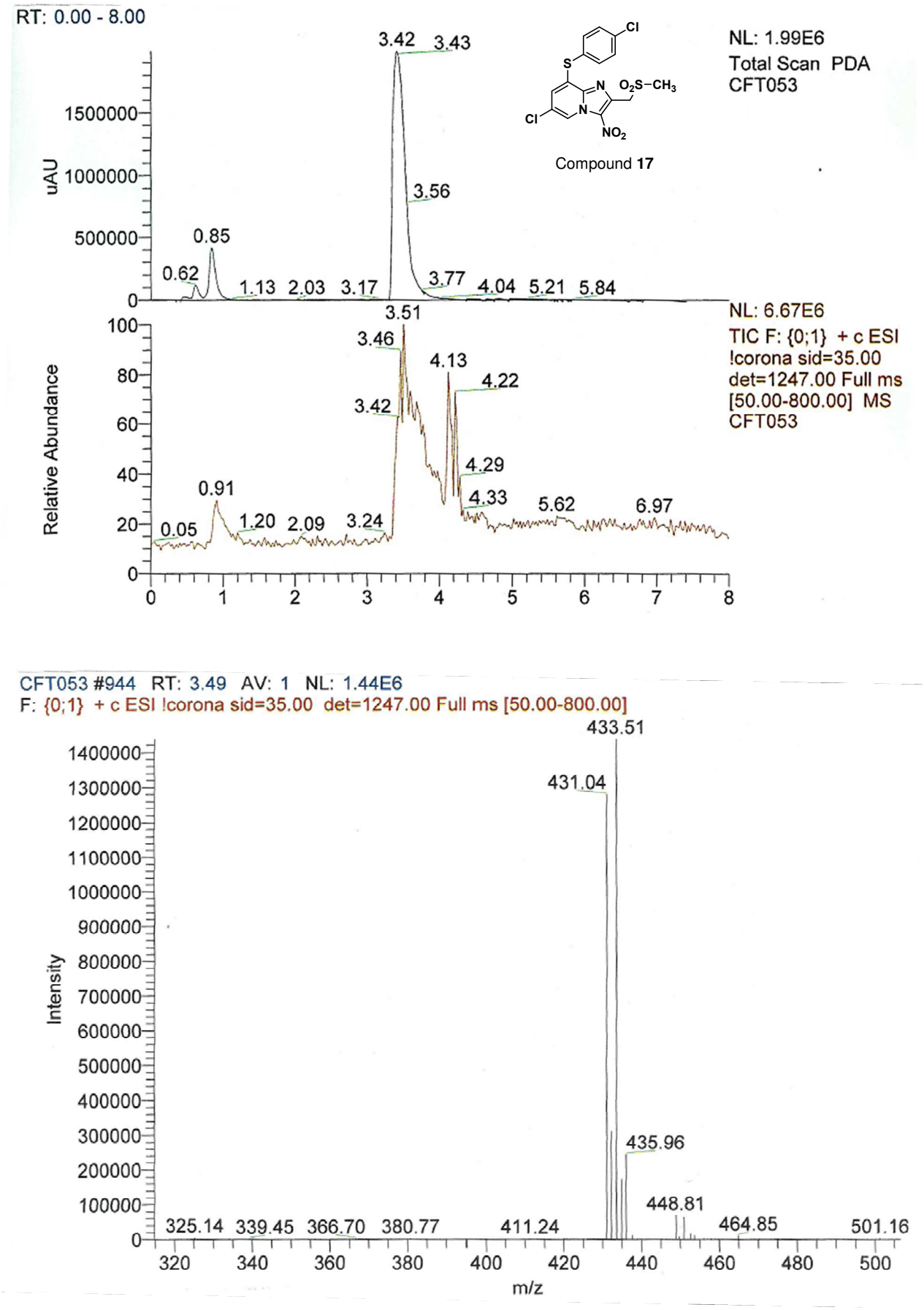

Figure S24 – LC/MS spectrum of compound **17**.

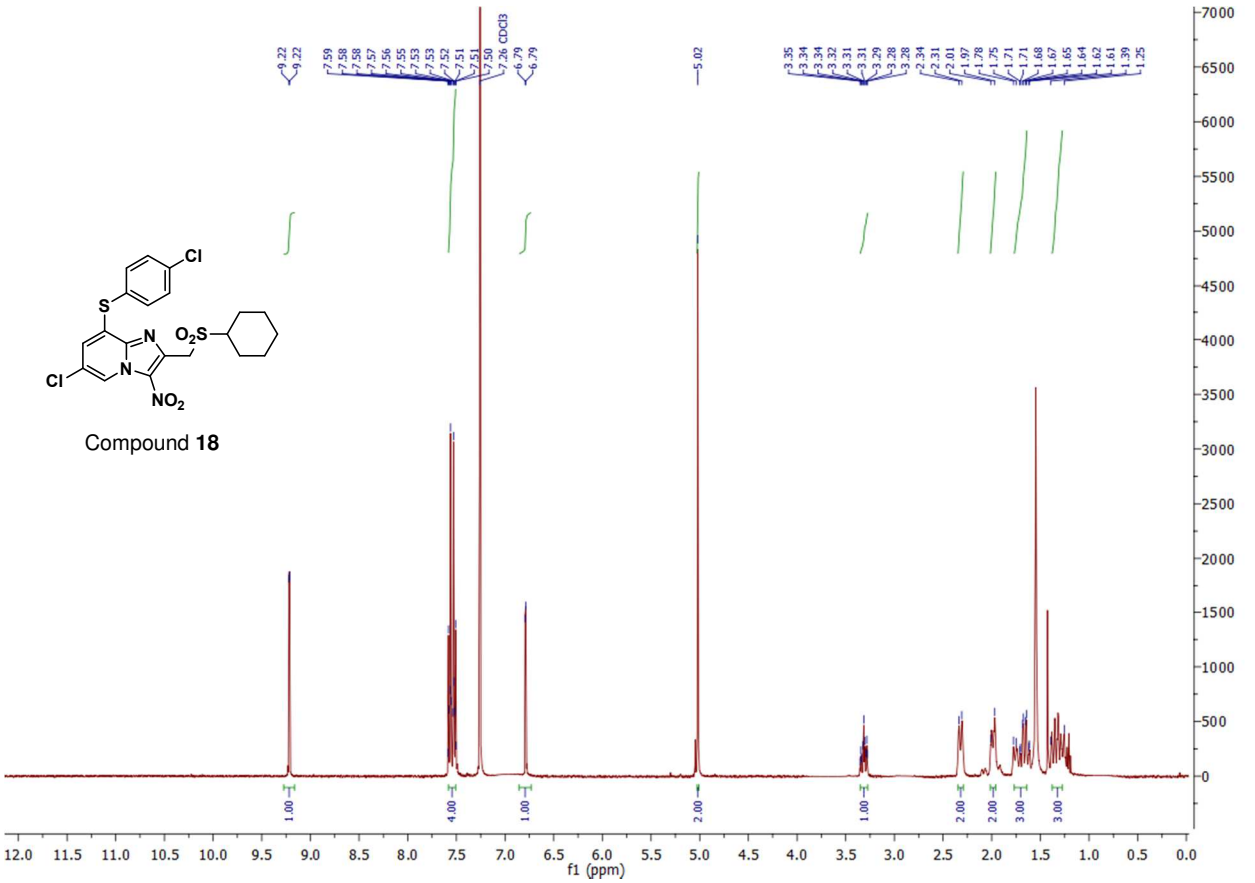

Figure S25 – ^{1}H NMR spectrum of **18** in $CDCl_3$, on a Bruker Avance III nanobay 400.

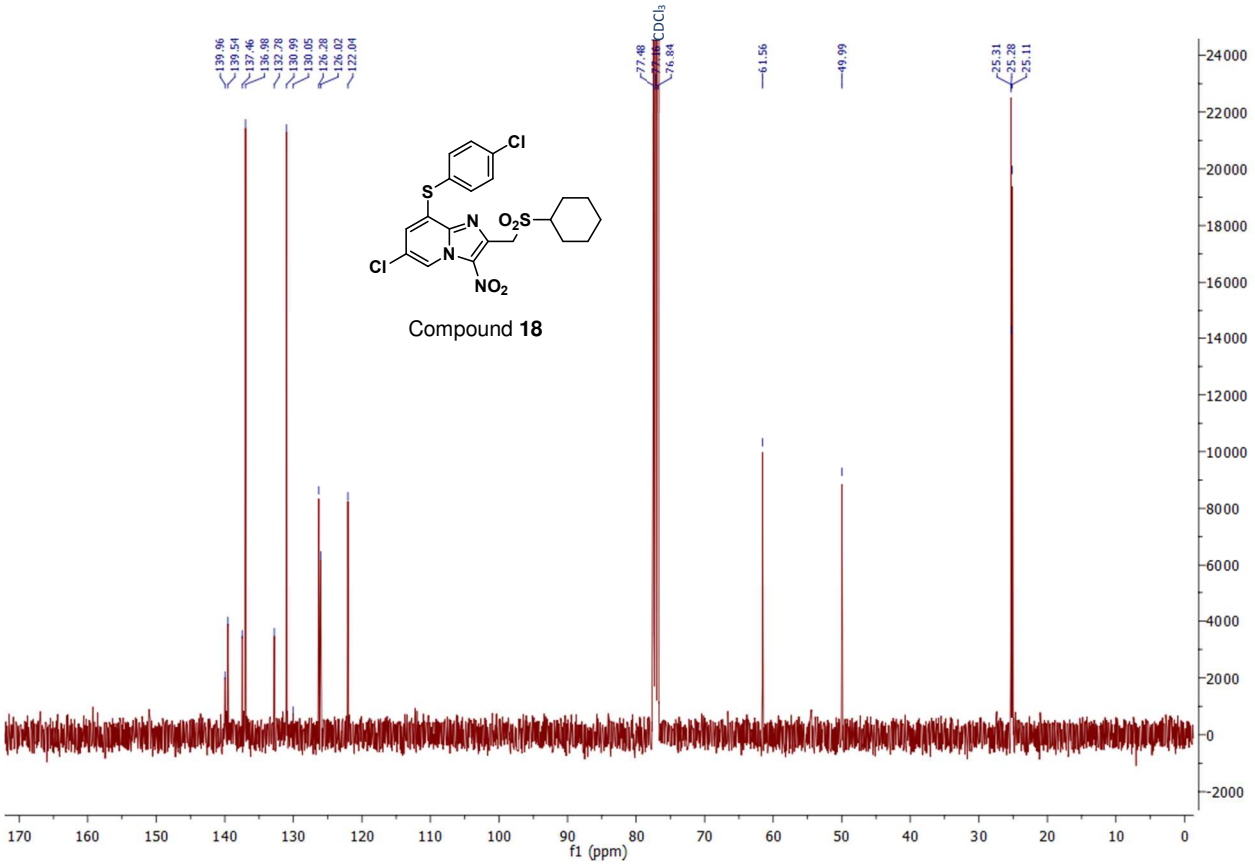

Figure S26 – ^{13}C NMR spectrum of **18** in $CDCl_3$, on a Bruker Avance III nanobay 400 spectrometer.

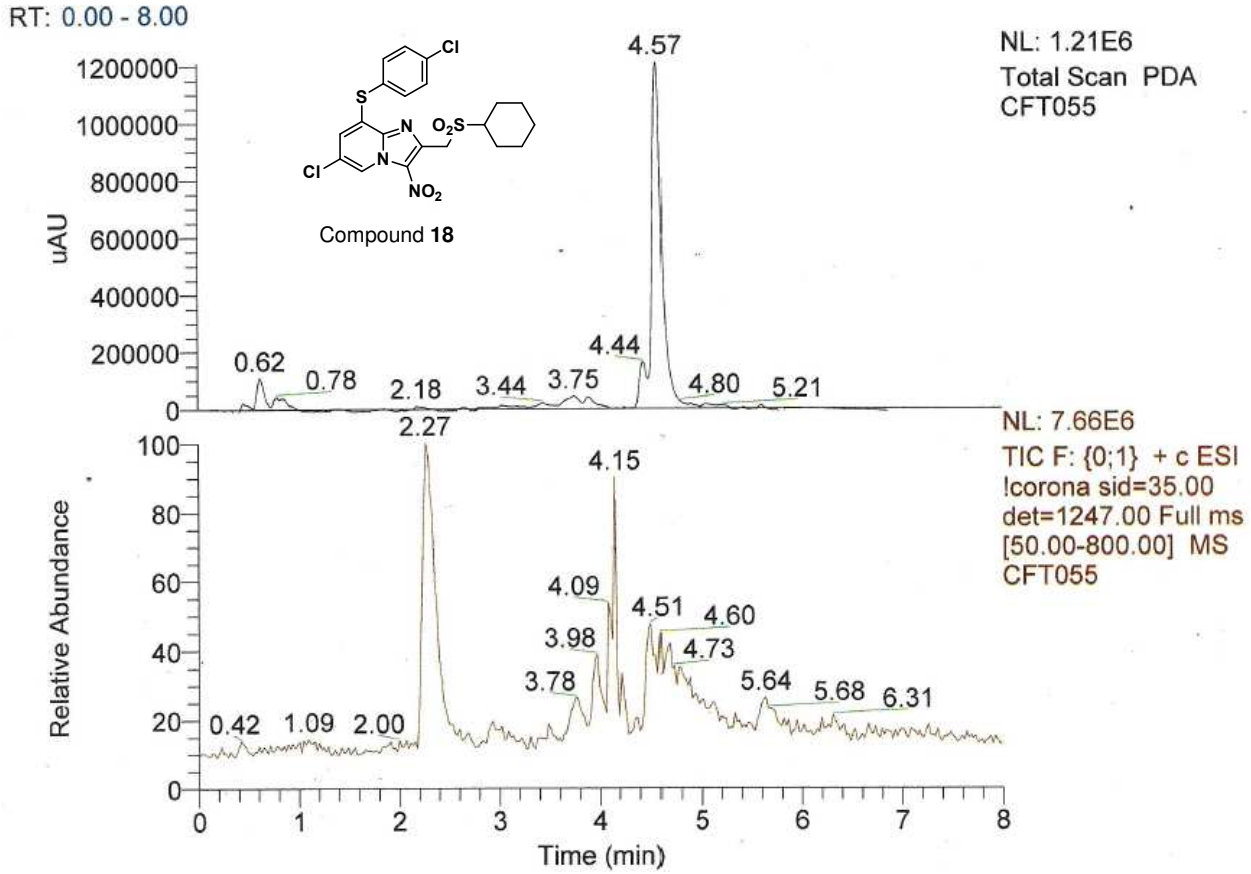

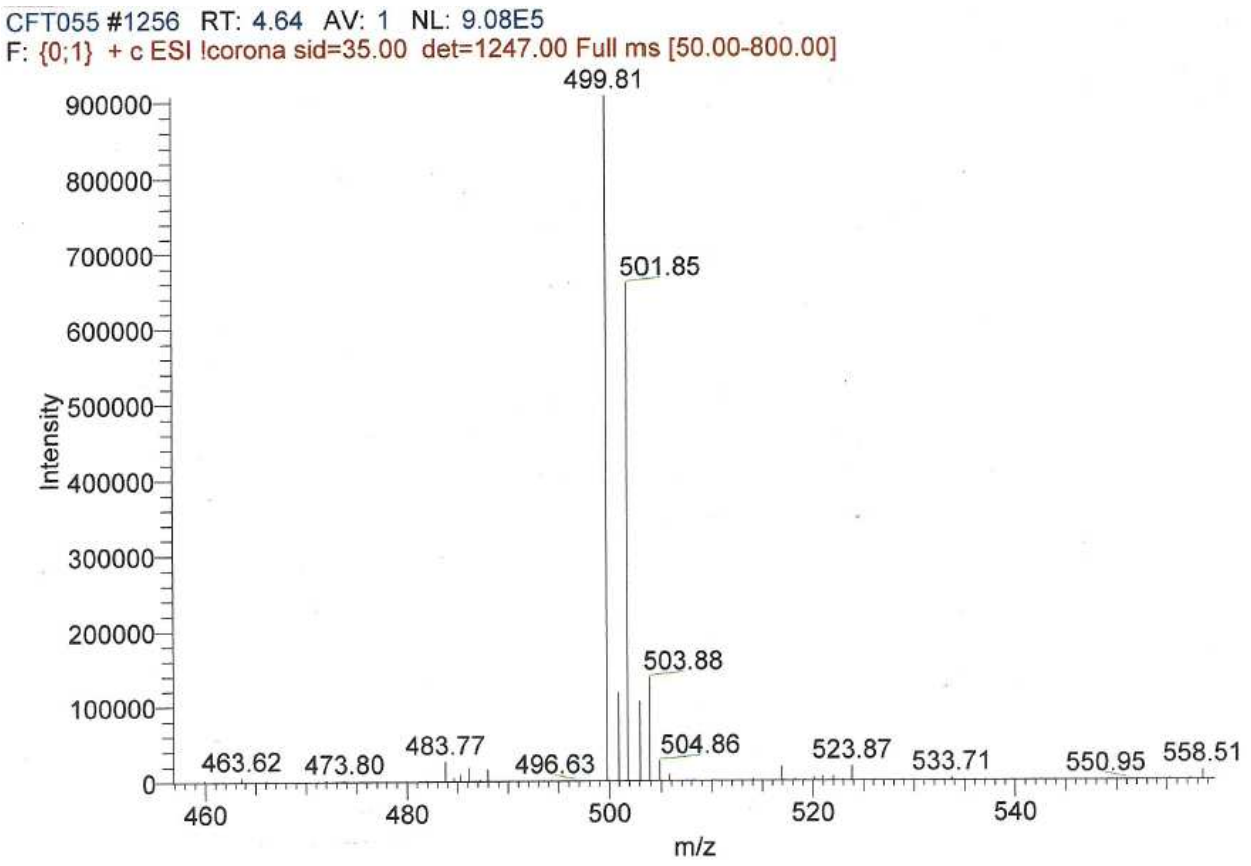

Figure S27 – LC/MS spectrum of compound **18**.

2. Microsomal stability and plasma protein binding assays

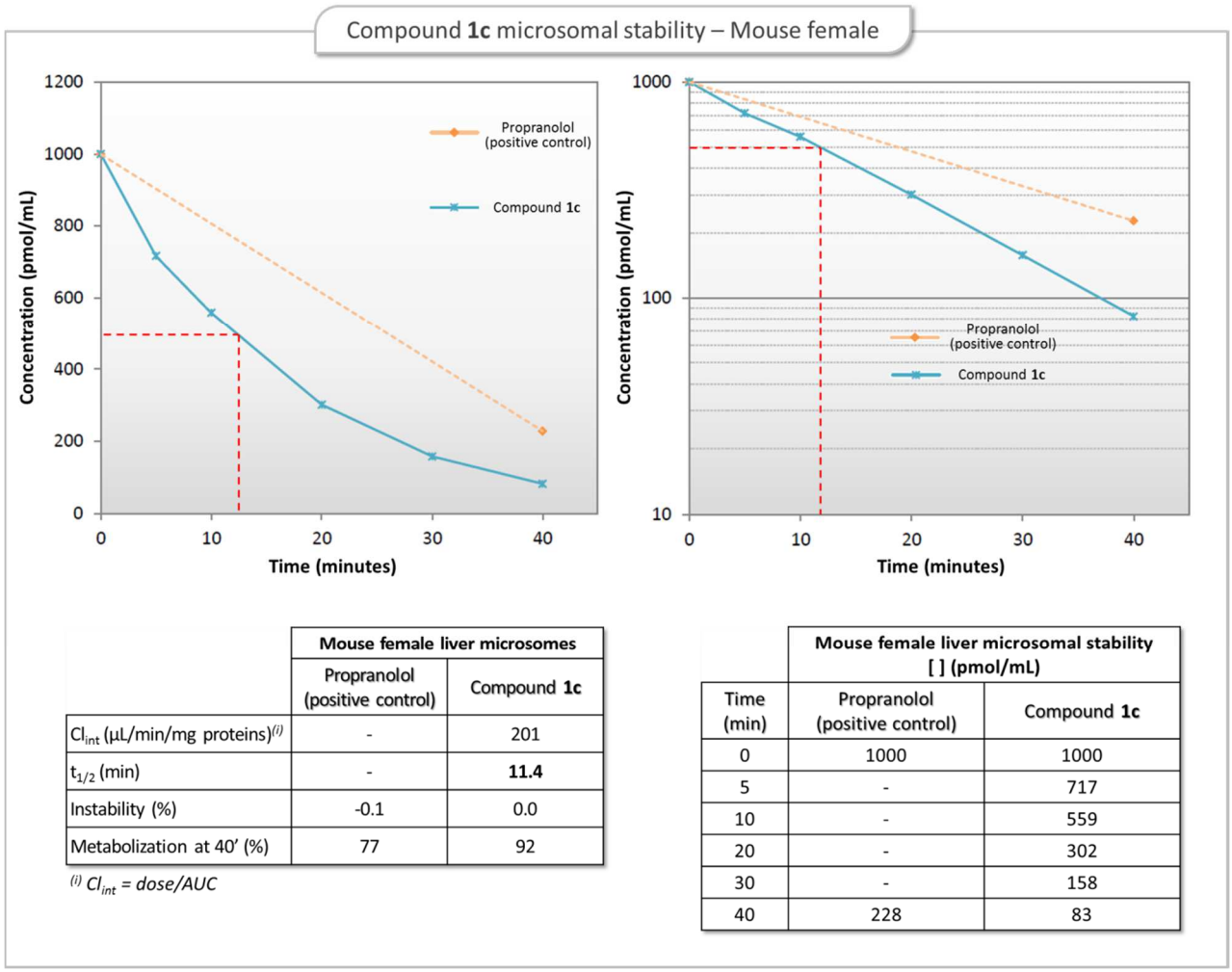

	Mouse female liver microsomes	
	Propranolol (positive control)	Compound **1c**
Cl_{int} (µL/min/mg proteins)[(i)]	-	201
$t_{1/2}$ (min)	-	**11.4**
Instability (%)	-0.1	0.0
Metabolization at 40' (%)	77	92

[(i)] Cl_{int} = *dose/AUC*

	Mouse female liver microsomal stability [ ] (pmol/mL)	
Time (min)	Propranolol (positive control)	Compound **1c**
0	1000	1000
5	-	717
10	-	559
20	-	302
30	-	158
40	228	83

Figure S28 – Microsomal stability results for compound **1c**.

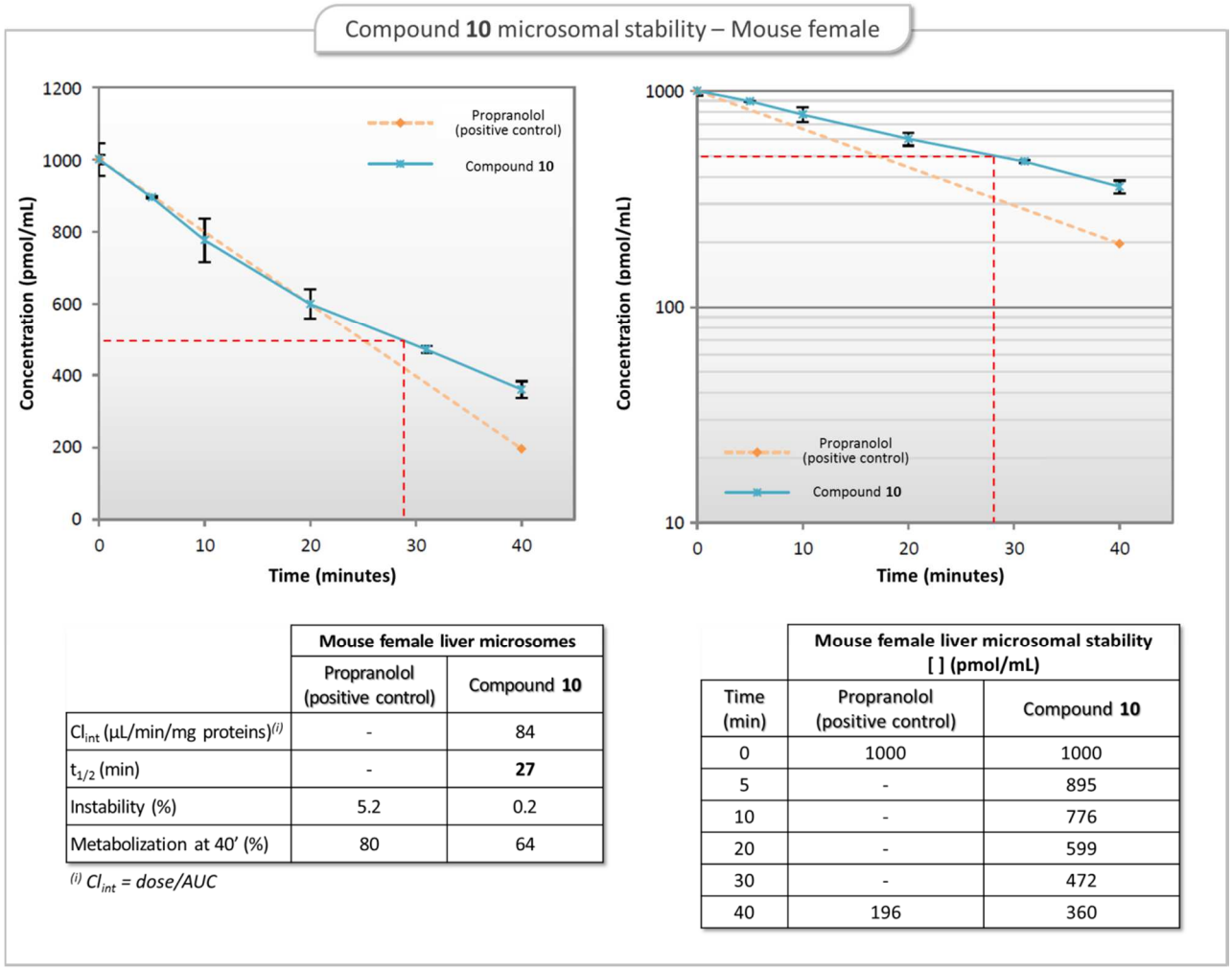

	Mouse female liver microsomes	
	Propranolol (positive control)	Compound **10**
Cl_{int} (µL/min/mg proteins)[(i)]	-	84
$t_{1/2}$ (min)	-	**27**
Instability (%)	5.2	0.2
Metabolization at 40' (%)	80	64

[(i)] Cl_{int} = *dose/AUC*

	Mouse female liver microsomal stability [ ] (pmol/mL)	
Time (min)	Propranolol (positive control)	Compound **10**
0	1000	1000
5	-	895
10	-	776
20	-	599
30	-	472
40	196	360

Figure S29 – Microsomal stability results for compound **10**.

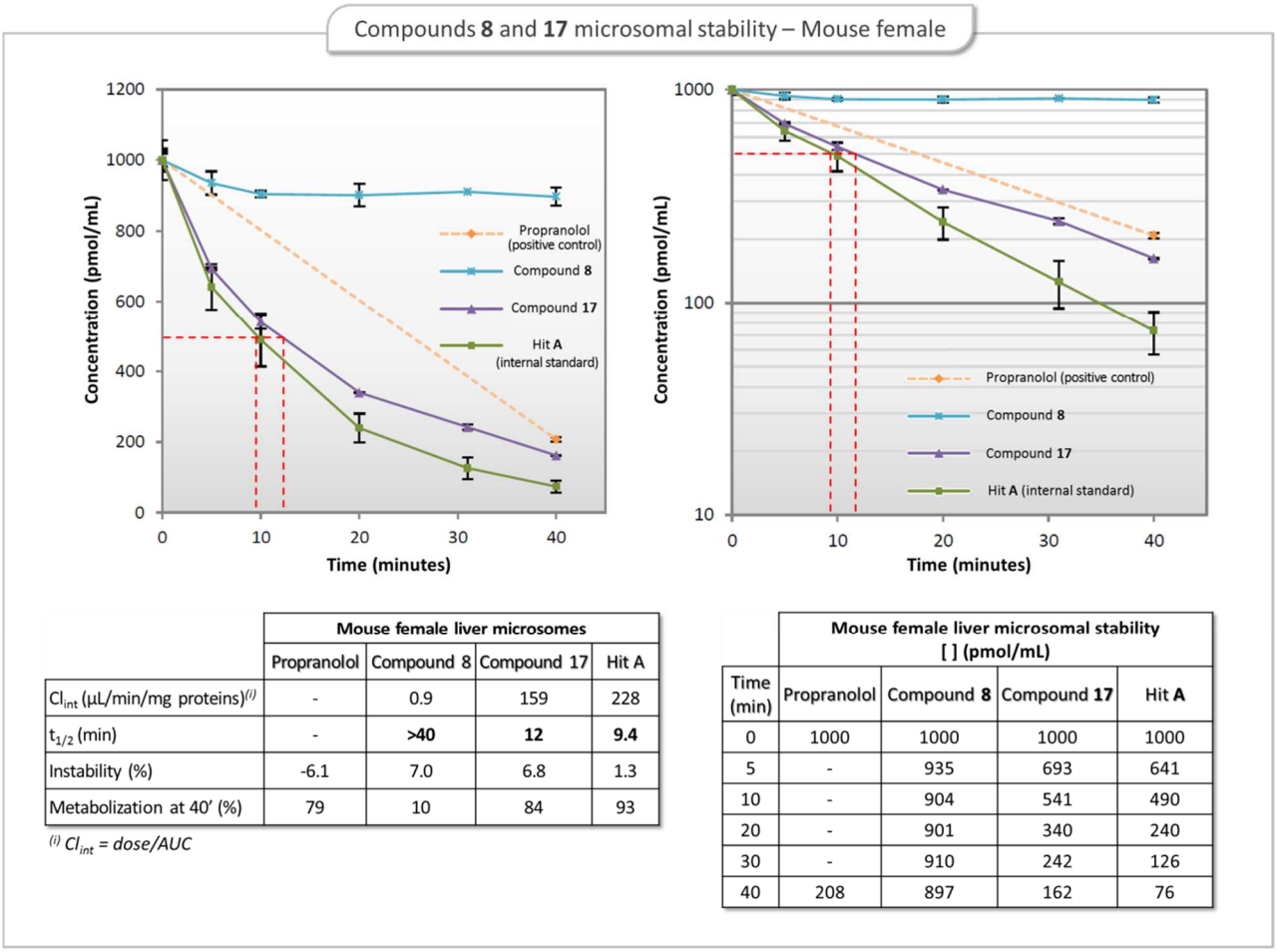

	Mouse female liver microsomes			
	Propranolol	Compound 8	Compound 17	Hit A
Cl_{int} (µL/min/mg proteins)[(i)]	-	0.9	159	228
$t_{1/2}$ (min)	-	**>40**	**12**	**9.4**
Instability (%)	-6.1	7.0	6.8	1.3
Metabolization at 40' (%)	79	10	84	93

[(i)] Cl_{int} = *dose/AUC*

	Mouse female liver microsomal stability [ ] (pmol/mL)			
Time (min)	Propranolol	Compound 8	Compound 17	Hit A
0	1000	1000	1000	1000
5	-	935	693	641
10	-	904	541	490
20	-	901	340	240
30	-	910	242	126
40	208	897	162	76

Figure S30 – Microsomal stability results for compounds **8** and **17**.

Compound	Buffer chamber	Plasma chamber	Ratio plasma $_{t=0}$	Ratio plasma $_{t=4\,h}$	Ratio buffer $_{t=4\,h}$	Recovery (%)	fu				% Binding
	Ratio	Ratio	Value	Average	Average	Value	Value	Average	Sd	CV	Value
Diclofenac (reference)	0.0014	0.4504	0.4234	0.45200	0.00120	107	0.00311	0.00266	0.00079	29.7	**99.73**
	0.0014	0.4478					0.00313				
	0.0008	0.4577					0.00175				
1c	0.0810	2.2695	3.4575	2.23393	0.07923	69	0.03569	0.03546	0.00023	0.6	**96.45**
	0.0806	2.2723					0.03547				
	0.0761	2.1600					0.03523				
8	0.2607	1.1072	1.7729	1.11950	0.2586	89	0.2355	0.23100	0.00720	3.1	**76.90**
	0.2611	1.1115					0.2349				
	0.2539	1.1399					0.2227				
17	0.0164	1.5964	1.5113	1.54483	0.01707	104	0.01027	0.01106	0.00069	6.3	**98.89**
	0.0167	1.4752					0.01132				
	0.0181	1.56290					0.01158				

Figure S31 – Plasma protein binding assay results of compounds **1c**, **8** and **17**.

3. Parallel Artificial Membrane Permeability Assay (PAMPA)

Compound	Concentration	Pe (nm/s)	logPe	Conclusion
8	100 µM	84.2 ± 2.9	1.93 ± 0.02	Diffuses moderately
Theophylline	250 µM	4.7 ± 0.6	0.67 ± 0.06	Does not diffuse
Corticosterone	100 µM	130.3 ± 7.1	2.11 ± 0.02	Diffuses

Figure S32 – Study of the passive diffusion of compound **8** through the BBB by the PAMPA assay.

4. Micronucleus assay

Test without S9 mix		Proliferation index				Micronucleated cell rates ‰			
		BI	MONO	CBPI	CI%	MNC1	MNC2	MNC-M	P
Control		436	64	1.86	-	8	11	9.5 ± 2.1	-
Solvent control		428	72	1.85	1.1	9	10	9.5 ± 0.7	-
Mitomycin C control		432	68	1.86	0	28	34	31 ± 4.2	<0.001
Compound **8**	0.01 mM	424	76	1.85	1.1	10	12	11 ± 1.4	>0.05 NS
	0.05 mM	419	81	1.84	2.3	9	11	10 ± 1.4	>0.05 NS
	0.1 mM	398	102	1.80	6.9	8	12	10 ± 2.8	>0.05 NS
	0.5 mM	392	108	1.78	9.3	8	10	9 ± 1.4	>0.05 NS

Test with S9 mix		Proliferation index				Micronucleated cell rates ‰			
		BI	MONO	CBPI	CI%	MNC1	MNC2	MNC-M	P
Control		433	67	1.86	-	9	12	10.5 ± 2.1	-
Solvent control		429	71	1.86	0	9	11	10 ± 1.4	-
Benzo[*a*]pyrene control		423	77	1.85	1.1	27	23	25 ± 2.8	<0.001
Compound **8**	0.01 mM	431	69	1.86	0	9	13	11 ± 2.8	>0.05 NS
	0.05 mM	411	89	1.82	4.6	10	12	11 ± 1.4	>0.05 NS
	0.1 mM	408	92	1.81	6.9	10	11	10.5 ± 0.7	>0.05 NS
	0.5 mM	404	96	1.81	6.9	9	12	10.5 ± 2.1	>0.05 NS

BI : Binucleated cells
MONO : Mononucleated cells
CBPI : Cytokinesis-Blocked Proliferative Index
CI% : Cytostasis index expressed in percentage as compared to the control

MNC1, MNC2: Micronucleated cell rates
MNC-M : Means of the micronucleated cell rates
P : probability of the chi-squared test ($p < 0.05$: significant difference as compared to the control culture)
NS : non-significant difference as compared to the control culture

Figure S33 – Micronucleus assay results for compound **8**, without metabolic activation and with S9mix.

5. Comet assay

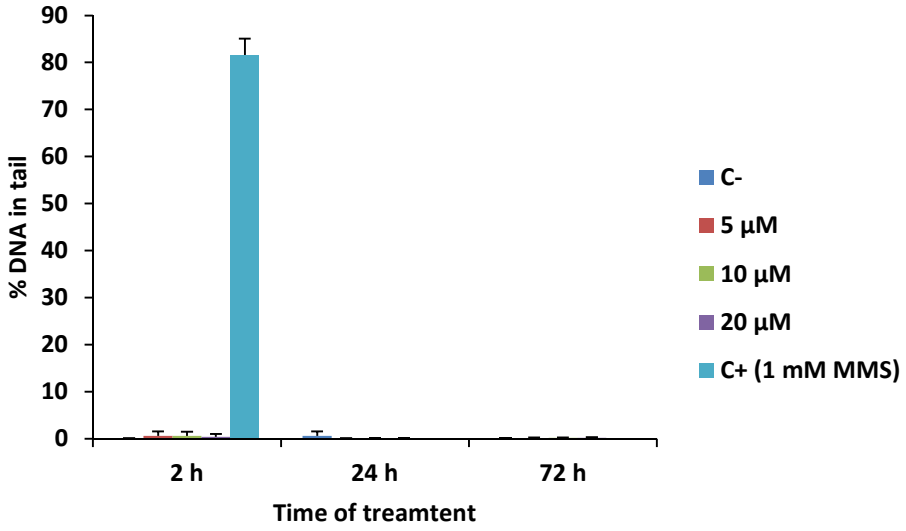

Figure S34 - % DNA in tail obtained in HepG2 cells treated with compound **8** at 0, 5, 10 or 20 µM for 2, 24 or 72 h. Cell treated with 1mM MMS for 2 h was used as positive control. Mean and SD of 3 independent experiments are shown.

6. Electrochemistry

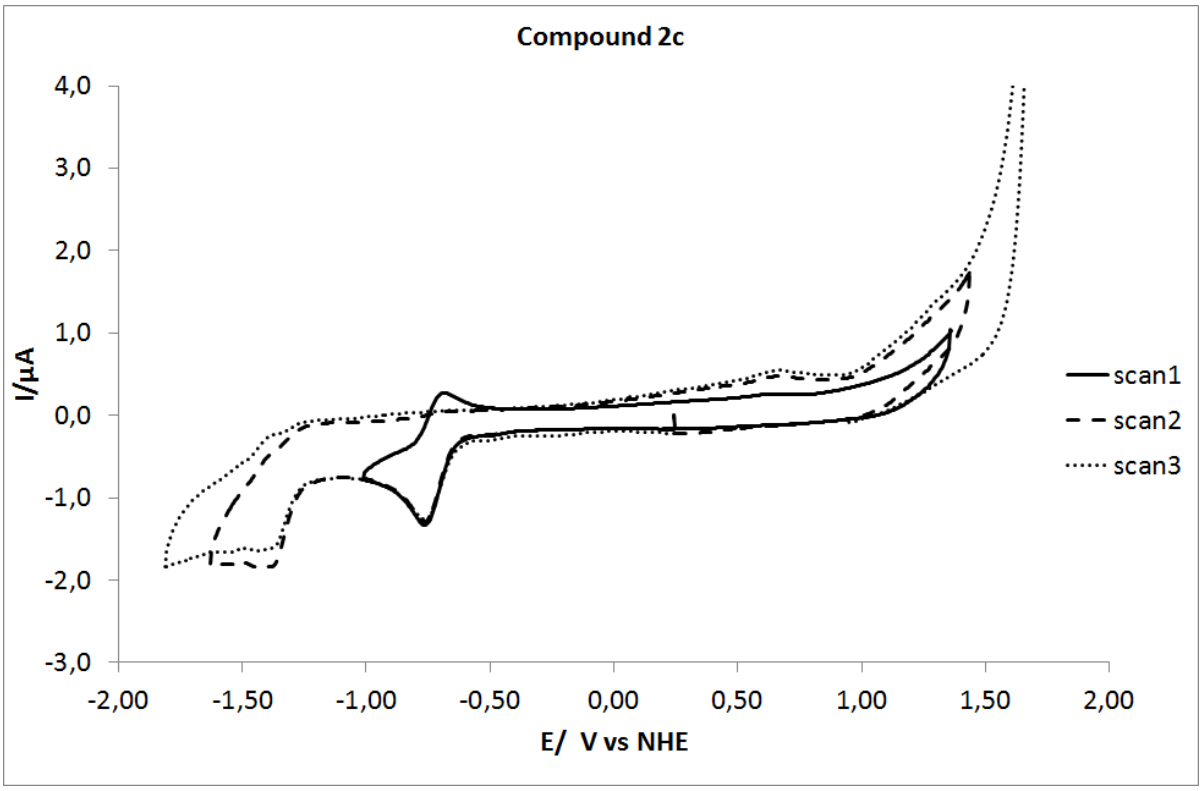

Figure S35 – Cyclic voltammetry of the compound **2c** (10^{-3} mol L^{-1}) in DMSO + 0.1 mol L^{-1} of (n-Bu_4N)[PF_6] on GC microdisk (r = 0.5mm) at room temperature. Scan rate: 0.2 V s^{-1}.

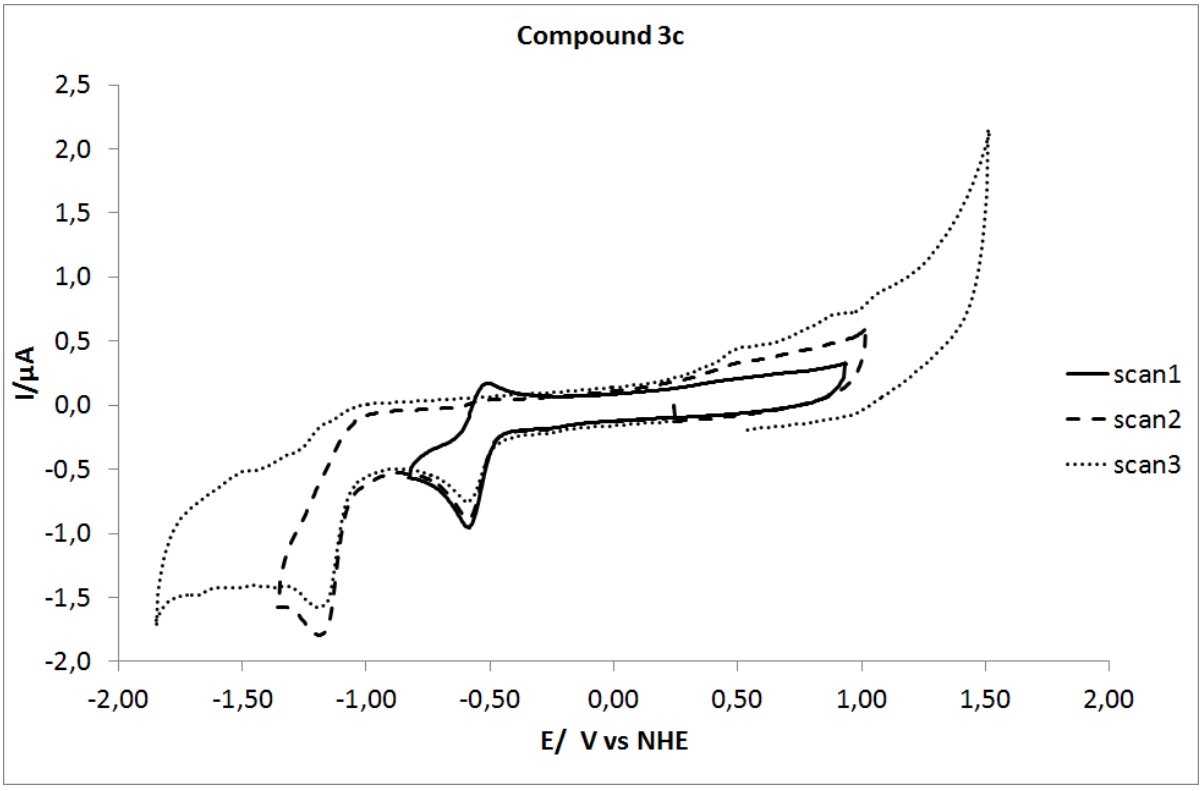

Figure S36 – Cyclic voltammetry of the compound **3c** (10^{-3} mol L^{-1}) in DMSO + 0.1 mol L^{-1} of (n-Bu_4N)[PF_6] on GC microdisk (r = 0.5mm) at room temperature. Scan rate: 0.2 V s^{-1}.

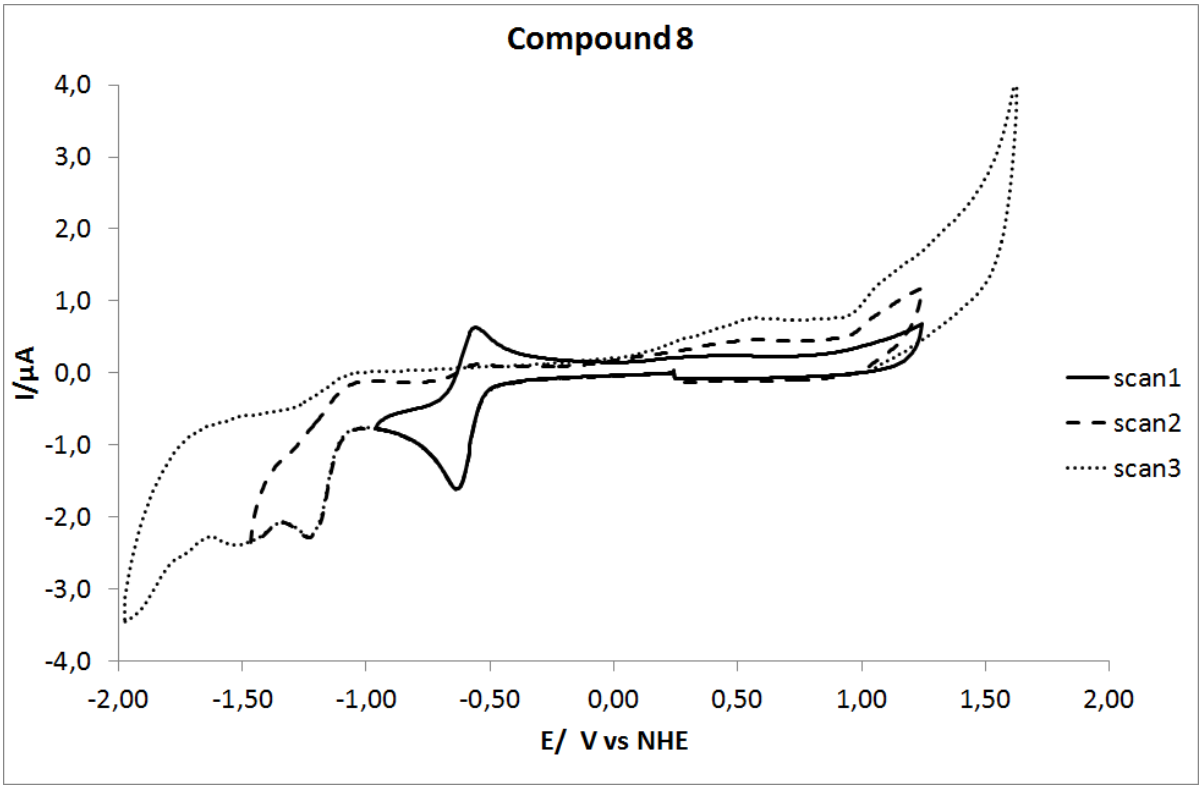

Figure S37 – Cyclic voltammetry of the compound **8** (10^{-3} mol L^{-1}) in DMSO + 0.1 mol L^{-1} of (*n*-$Bu_4N)[PF_6]$ on GC microdisk (r = 0.5mm) at room temperature. Scan rate: 0.2 V s^{-1}.

7. *In vivo* pharmacokinetics parameters

Cmpds	Retention time (min)	Precursor ion		Product ion					
				Quantitation			Confirmation		
		m/z	Q1 pre-bias (V)	m/z	Collision energy (V)	Q3 pre-bias (V)	m/z	Collision energy (V)	Q3 pre-bias (V)
8	2.38	367.8	-21	243.05	-24	-16	189.8	-43	-11
							321.9	-15	-25
Ornidazole (IS)	2.0	220	-30	82	-30	-14	128.1	-15	-27

Figure S38. LC retention time (RT) and selected MS/MS detection conditions.

		LLOQ 5 ng/mL	LQC 10 ng/mL	MQC 75 ng/mL	HQC 625 ng/mL	1.5 × ULOQ 1500 ng/mL
Coefficient of determination (r^2)				0.9962 ± 0.0038		
Recovery (%CV) *(n = 3)*		91.3% (13.7%)	86.8% (12.4%)	97.1% (2.6%)	92.1% (6.6%)	
Intra-assay *(n = 5)*						
	Mean ± SD (ng/ml)	4.89 ± 0.66	9.46 ± 1.24	73.60 ± 1.98	598.51 ± 42.99	
	Accuracy	97.7%	94.6%	98.1%	95.8%	
	CV%	13.4%	13.1%	2.7%	7.2%	
Inter-assay *(n = 5)*						
	Mean ± SD (ng/ml)	4.87 ± 0.29	10.74 ± 0.48	75.02 ± 6.36	649.0 ± 45.06	
	Accuracy	97.7%	107.4%	100.0%	103.8%	
	CV%	6.0%	4.4%	8.5%	6.9%	
Dilution test *(n = 3)*						
1.25-fold dilution	Mean ± SD (ng/ml)			76.88 ± 7.45	597.13 ± 31.0	
	Accuracy (%CV)			102.5% (9.7%)	95.5% (5.2%)	
2-fold dilution	Mean ± SD (ng/ml)			72.70 ± 6.67	589.01 ± 11.63	1499.6 ± 185.2
	Accuracy (%CV)			96.9% (9.2%)	98.0% (5.5%)	100.0% (12.3%)
4-fold dilution	Mean ± SD (ng/ml)			71.09 ± 4.12	467.72 ± 78.48	
	Accuracy (%CV)			94.8% (5.8%)	74.8% (16.8%)	

SD: standard deviation ; CV: coefficient of variation

Figure S39. Main parameters of the validation protocol for whole blood dosing of compound **8**.